

Dear Editor,

please find attached a revised version of the paper: Constraining the ship contribution to the aerosol of the Central Mediterranean. We have addressed all the questions raised by the reviewers, and I hope now it can be published on ACP.

I want to thank both reviewers for their constructive comments and suggestions. Please find below the detailed answers. All authors concur with the submission of the revised paper

Best regards,



Answer to the reviewers' comments

Anonymous Reviewer #1

Dear Editor,

this manuscript presents an assessment of shipping contributions to PM10 aerosols in two locations in the Mediterranean Sea. It presents a very interesting integrated approach combining different tools such as analysis of the chemical composition of PM10, tracer analysis, back-trajectories and ship inventories and databases. Whereas certain of these tools are not novel and suffer from limitations (e.g., tracer methods), the combination of all of them provides very interesting results. Over all, the paper is of interest to the scientific community and merits publication after revision.

Specific comments are provided below:

- lines 110-113 would fit better in the Methods section

Figure 1 and the corresponding text were moved to the methods section as suggested.

- line 276: very good, it is very important that the authors highlight this kind of limitation.

- line 292: "smaller" should be "lower". In general, the English is correct but a review by a native speaker would be helpful.

The sentence was corrected. The paper was revised by a native English speaker.

- Figure 2: the nitrate contribution at LMP is surprisingly high, considering the thermal instability of this species. Can this be due to an artefact or high uncertainty of the measurements?

The nitrate concentrations measured in this campaign are in agreement with the long term measurements performed at Lampedusa (e.g., Calzolari et al., 2015) and with data from other remote sites in the western (Mallorca; e.g. Simo et al., 1991) and eastern Mediterranean (Finokalia; e.g. Mihalopoulos et al., 1997). The presence of artefacts in the nitrate sampling are documented in literature. These artefacts cause lower concentrations in the sample than in the atmosphere, in polluted regions due to NH₄NO₃ volatilization

deposited on the filter. We believe that in relatively clean conditions like those incurring in Lampedusa and Capo Granitola the impact of artefacts is small, and the derived values are reliable. These values also suggest that ship emissions may play a large role. A comment was added to the text.

- line 340: also, EC concentrations are much higher in CGR, supporting this interpretation (the dominance of anthropogenic sources of carbonaceous aerosols in CGR)

We agree with the reviewer (see also comment 11 of reviewer 2). The sentence was changed and the differences were discussed.

- Figure 4 is interesting but not so useful, it could be removed if the authors encounter space limitations

We agree with the reviewer; the discussion of the sea breeze is interesting, but not directly related with the paper main topic. We delete this part from the manuscript.

- line 402: about the representativeness of this kind of ratios: it should be stated that this ratio may have a large variability due to varying fuel composition and engine operating conditions

We agree with the reviewer. The sentence was modified.

- line 424: LCR=1-5, how specific are these values for the specific refinery in the Moreno et al study? Can they really be extrapolated to other refineries? What can the uncertainty be for other refineries? Please discuss

Section 3.1.2 was largely modified, also taking into account the different comments of the reviewers.

The discussion on the LCR variability was improved and new references to support the discussion were added. In particular, we have reported range of values for ship, refinery, and crustal components of the aerosols, also with reference to literature results.

- line 430: 24% of samples with LCR>1 and 8% >2, this is a very high contribution (32%), can the contribution from refineries be so high at LMP? From where? Or is this an example of the limitation mentioned above, the uncertainty of these LCR values when applied to other study areas? Please discuss

We have double checked the calculated LCR values. As correctly suggested by reviewer 2 (see his/her point 13), we did not take into account the uncertainty and the detection limit of La and Ce measurements. The instrumental detection limit on these determinations was added in section 2.1. The very high values of LCR correspond with very low, in some cases below the detection limit, La and/or Ce concentrations. In these cases the uncertainty on LCR exceeds 100%. The elimination of these data points filters out most of the very high LCR values. We have thus redrawn Figure 5 (that becomes fig 4) accordingly, also indicating the range of values which are expected for the crustal component.

- Figure 6: again, the authors show only one point per type of dust, what is the uncertainty? The authors' results seem very conclusive with regard to their own samples, but it would still be useful

to see the potential variability in the other (refinery, UCC) types of dust. If no other data is available for this kind of sources, please mention as a limitation

The Lanthanoid content in Saharan dust measured in several aerosol size classes and from different areas of Sahara, as well for other compounds are reported in figure 6 (figure 5 in the revised version). The discussion on the variability of the composition was expanded (see also answer to the two previous comments).

- line 575: it is also possible that this is due to the larger aerosol dilution during transport towards LMP?

We agree with the reviewer. Dilution may be a cause of lower V concentration at LMP. A sentence on the possible role of dilution was added

- line 666: "two times higher than...", isn't this strongly dependent on fuel and engine operating conditions?

We agree. The sentence was changed accordingly.

- line 702: "component" should be "components"

The typo was corrected.

- line 703: the term "rough estimate" is more adequate than the "unambiguous identification" used in other parts of the text

In the text we use "rough estimation" referring to the quantitative estimation of the minimum contribution of ship aerosol (i.e., using the method of the minimum values reported in section 3.4). However, we believe that the combination of the different methods discussed in the paper leads to an unambiguous attribution of the measured aerosol to the ship source.

- line 722: "50%", again, this is very variable depending on engine conditions, meteorology (oxidation rate of SO₂...), etc. Therefore this 20% difference can be expected

We agree. This is one of the reasons why we may estimate only the lower limit for sulfate contribution. The sentence was corrected.

- line 741: the higher % contributions obtained should not be considered a negative result, due to the potentially large variability of these contributions. It is correct to compare the order of magnitude with the previous literature, but the precision of the authors' method (and of other currently available methods) is not sufficient for them to carry out a detailed comparison of the results obtained. The results presented are quite positive, in my opinion.

We fully agree. The sentence is explaining possible reasons for the observed differences.

- line 781: should "as expected", be added at the start of the sentence?

We agree with the reviewer's comment, and added "as expected" at the beginning of the sentence.

Anonymous Reviewer #2

This is a nice work that attempts to provide some estimates of the contribution of ship emissions to the budget of specific chemical species as well as to PM10 in total. There is undoubtedly quite a large fraction of uncertainty into this, as the authors themselves admit and partly discuss, which is based not only on the methodological limitations but also on the short period of this study and the very specific spatial grid they are referring at. In this line, even though I recognize some weakness of the paper to provide substantial new concepts, ideas or methods (as required by ACP), I still see the importance of such local studies in a hot issue like ship emissions in the Mediterranean and support its appropriateness for publication in the CHARMEX SI. I am suggesting major revision mainly because I would like to urge the authors to reorganize the presentation of their results in a way that they show up better the important aspects coming out of it.

General comment:

As the authors mention in lines 704-706, the use of their results(they are referring to the V different ratios but this is transferred also to the rest of the analysis) is limited by the fact that they refer to specific meteorology, photochemistry, space and season. This is obvious and unavoidable, but still there should be some discrimination of what is indeed only of local interest and what could be somewhat generalized e.g. by using ranges of values, relations with the level of traffic, or better describing the sensitivity of those results and comparing them more detailed with existing literature (even their own previous work).

We only partly agree with the comments on the local nature of the study. Of course, the analysis refers to a specific region, meteorology, season, etc. However, we believe that the information we retrieve is sufficiently robust, and relevant on a larger scale than local, mainly because it is based on two sites with markedly different characteristics. In particular, the site of Lampedusa is relatively far from the main shipping route, and the observations there suggest that ship emissions impact the Mediterranean basin on a larger scale than local. We have however added some comments and references with the aim of placing the obtained results in a wider perspective.

Moreover, the structure of the paper, at some point, confused me by means that I was expecting a number of synergistic analyses to identify and discriminate ship emissions (e.g. the standard markers, then some improvement by rare earth elements, then further refinement via trajectories etc), while Figure 8 speaks for itself! The authors might like to start from Fig. 8 and then provide further proof or try to explain discrepancies e.g. between the two sites. My overall impression is that the paper started from V and after a loop of some necessary and some unnecessary steps it ends up again with V. I hope some of my more specific comments that follow will help authors make improvements to the manuscript.

We agree that links among the different parts of the analysis are lacking or have been poorly discussed. However, we believe that including these lacking links the logical structure of the paper is sound, and we did not change the overall structure of the paper in the revised version. We have explained in more detail the connections among the different analyses, and the way in which they affect data. Some parts were heavily reorganized (see e.g., section 3.1.2), and some non essential information was removed (e.g., figures 4). We believe that the presentation is now clearer, and thank the reviewer for this suggestion.

Specific comments:

1. *The language is very clear to understand but it should definitely benefit from some native English speaker editing.*

The paper was revised by a native English speaker.

2. *The word "anthropic" is probably misused instead of "anthropogenic". This is not based on the frequency of use of the words in the relevant literature, but mainly on the meaning of "anthropic" which is more what is influenced by humans or taking place during human era, rather than what is generated by human activities. I see its use mainly in social sciences. In Greek they use the translation of the word anthropogenic and not anthropic to refer to sources or pollution (in any case they are both Greek words!).*

We agree with the comment. We have checked the use of the terms "anthropic" and "anthropogenic" throughout the paper.

3. *Part of the paragraph in lines 100-118 seem to fit better as introduction to section 2.1. That would also include Fig.1 and the description of the sites. I would suggest to keep in the introduction only the nice unfolding of the diachronically followed strategy.*

Figure 1 and the text were moved to section 2.

4. *In section 2.1 (lines 146-153) there is a great number of references to available measurement types at Lampedusa that seem irrelevant to the specific work. Only references contributing to the description of Lampedusa characteristics as a site should be included here.*

The number of references was reduced as suggested.

5. *In section 2.1 there is a lot of information about the techniques used in the two stations. Probably the authors would like to organize part of this info in a table, to help readers follow easier.*

A table with the sampling strategy and measurements carried out on each filter was added.

6. *Please add information on start-end times of the 12h sampling at the two sites. See e.g. line 172, what is meant by diurnal sampling?*

The start and end sampling time was added in the text and in the table reporting the sampling strategy.

7. *Section 2.3 (lines 228-232). Please check on Solomos et al. 2015 who are articulating improvements in resolving and forecasting the dispersion of smoke plumes, in their case, over particularly complex terrains (including BL and sea-breeze system particularities), by incorporating high-resolution (spatial and temporal) meteorology and satellite data. (Solomos S., V. Amiridis, P. Zanis, E. Gerasopoulos, F.I. Sofiou, T. Herekakis, J. Brioude, A. Stohl, R.A. Kahn, C. Kontoes, Smoke dispersion modeling over complex terrain using high resolution meteorological data and satellite observations – The FireHub platform, Atmospheric Environment, Volume 119, <http://dx.doi.org/10.1016/j.atmosenv.2015.08.066>.)*

A comment and the reference were added in the discussion.

8. Section 3.1 (lines 276-278). Could you here quantify this low crustal elements contribution as a percentage? (see lines 295-296).

The percentage of crustal content with respect to the total PM10 concentration was added.

9. Section 3.1 (lines 283-284). A reference should be provided.

The sentence applies to Lampedusa (or remote marine sites). This is now specified in the text.

10. Section 3.1 (lines 286-288). Though I understand the meaning, this sentence should be rephrased.

We agree. The sentence was rearranged.

11. Section 3.1 (lines 335-336, Fig. 3). I do not see this different behavior. At the same part of the plot which corresponds to lower values (see LMP axes) the behaviour seems similar – no specific correlation. So it is from a threshold and upwards that the influence of primary sources is shown on CGR. Please rearrange the interpretation.

We agree with the reviewer. Essentially, there are different concentration ranges at the two sites, and a correlation for moderate and elevated values at CGR. We have changed the sentence.

12. Section 3.1 (line 356, Fig. 4). On June 18 the diurnal cycle is opposite to what is described. (lines 359-362) This is not the case in all days ... could the authors identify the sea breeze influenced days on the plot?

The discussion of the evolution linked to sea breeze and coastal circulation, and the different daily evolutions go beyond the main objective of the paper. Figure 4 was consequently deleted in the revised version.

13. Section 3.1.2 (lines 429-432). The percentage for $LCR > 1$ at LMP seems large. How much is it biased by the fact that low La and Ce (especially Ce) values could produce arbitrary ratios? Please put a threshold to refine this analysis. Is this analysis with LCR used somehow to further constrain your statistical sample in the following parts? Or is it just to prove the appropriateness of V as a marker in this period? If so, what is the improvement brought in and how does it compare with the trajectories analysis?

We agree. The very high LCR values are discussed in the answer to reviewer 1 (see comment to line 430). The impact of the LCR values on the selected data was added, as well a discussion with respect to the trajectory analysis. The impact of LCR is shown in the following figures and in the dataset, and is discussed in the following parts of the paper. The cases with elevated values of LCR and possibly influenced by refineries have been highlighted also in figure 8 (figure 7 in the revised manuscript).

14. Section 3.2.1 (Fig. 7). The scale used in Figure 7 is probably not appropriate. I would avoid showing contributions lower than 1%, they take up most of the space in the plot without having anything to say about this. Choose the scale and probably the area to show, so that it fits to the local aspects that this part of the analyses addresses. How confident are you for the representation of the backtrajectories in the very short distances (few kilometers) and the such low altitudes (few hundred meters) between the trajectory starting points and the ship tracks? Once more, as in the previous comment, how it compares if e.g. you change the selection criteria, does it much the LCR results?.

We understand the reviewer's point but the purpose of Figure 7 (figure 6 in the revised version) was just to give an overview of the results of the trajectory analysis and to show the air masses origin on a continental scale rather than a local one, as a consequence of the prevailing weather regimes observed during the campaign (e.g. the relatively high frequency of air masses coming from Central and Western Europe, especially in June 2013 due to the numerous Mistral episodes). In fact, Section 3.2.1 serves as an introduction to the more detailed analysis focused on the local aspects, which is discussed in the following Section 3.2.2. Furthermore, we cannot fully agree that contributions lower than 1% take up most of the scale in the plot, therefore we would rather keep Figure 7 (now figure 6) unchanged.

As the Reviewer correctly points out, the calculation of backtrajectories in the lowest layers and at short distances from the starting point may be affected by substantial uncertainties. However, this is particularly true when using coarse meteorological fields from global models (resolution of order of 50 km in space and three or six hours in time). In the present study outputs from a mesoscale model with relatively high spatial resolution (10 km and 35 vertical levels) and hourly temporal resolution are used to drive trajectory calculations. Though for some more specific applications and in particularly complex topography areas even higher resolutions would be required, we believe that for the purposes of our study the quality of meteorological fields is more than adequate. Indeed, our main focus is the description of transport within the marine boundary layer, which is reasonably well described using a 10-km grid spacing.

15. Section 3.3 (Fig. 9). As far as I understood the authors have used a previous obtained value of 200 for $nssSO_4/V$, confirmed by this shorter study, and then calculated similar ratios for other species only from this study. It seems to me more like an eye approach which does not take into account the uncertainty of the points and the log scale used. Thus, the value of 10 NO_3/V could easily be 20 or 30. I would suggest a more thorough analysis on this, based on some logarithmic fitting and then extraction of a plateau value for higher V . Then give ranges based on the uncertainty and propagate the error into the final calculations that follow.

We agree with the reviewer that the limit ratio was determined arbitrarily.

In order to obtain a better estimate, we have tried to follow the reviewer's suggestion and have tried to fit different analytical curves to the data. However, we could not find a coherent fitting scheme for the different species, and ended up in choosing a simpler method. The limit ratio was calculated as the average of the observed values for $V > 15$ ng/m³.

This method allows to derive a quantitative estimate of the limit ratio, and to calculate its standard deviation.

Since we are determining a lower limit for the ship contribution to the total aerosol load, and a values of the ratio may still be decreasing for V around 15 ng/m³, we used for each species a limit value which is equal to the average minus one standard deviation.

These limit values are somewhat different at Lampedusa and Capo Granitola, and are reported in figure 9 (now figure 8) and discussed in the text.

16. Section 3.4. I think this is the part that my general comment should be mostly taken into account. Highlight what is of general interest than only of local impact and use; elaborate further on comparisons (e.g. like in lines 741-746).

We have expanded the discussion at the end of section 3.4. See also the answer to reviewer 2 general comment.

1 **Constraining the ship contribution to the aerosol of the Central** 2 **Mediterranean**

3
4 S. Becagli¹, F. Anello², C. Bommarito², F. Cassola^{3,4}, G. Calzolari⁵, T. Di Iorio⁶, A. di
5 Sarra⁶, J.L. Gómez-Amo^{6,7}, F. Lucarelli⁵, M. Marconi¹, D. Meloni⁶, F. Monteleone², S.
6 Nava⁵, G. Pace⁶, M. Severi¹, D. M. Sferlazzo⁸, R. Traversi¹, and R. Udisti¹

7
8 ¹ Department of Chemistry, University of Florence, Sesto Fiorentino, Florence, I-50019,
9 Italy

10 ²ENEA, Laboratory for Earth Observations and Analyses, Palermo, I-90141, Italy

11 ³Department of Physics & INFN, University of Genoa, Genoa, I-16146, Italy.

12 ⁴ARPAL-Unità Operativa CFMI-PC, Genova, I-16129, Italy.

13 ⁵Department of Physics, University of Florence & INFN-Firenze, Sesto Fiorentino,
14 Florence, I-50019, Italy.

15 ⁶ENEA Laboratory for Earth Observations and Analyses, Roma, I-00123, Italy

16 ⁷Department of Earth Physics and Thermodynamics, University of Valencia, Spain.

17 ⁸ENEA, Laboratory for Earth Observation and Analyses, Lampedusa, I-92010, Italy

18
19 **Keywords:** ship aerosol, Central Mediterranean Sea, PM₁₀, La-Ce ratio, Vanadium.

20 21 **Abstract**

22
23 PM₁₀ aerosol samples were collected during summer 2013 within the framework of the
24 Chemistry and Aerosol Mediterranean Experiment (ChArMEx) at two sites located North
25 (Capo Granitola) and South (Lampedusa Island), respectively, of the main
26 Mediterranean shipping route in the Sicily Channel.

27 The PM₁₀ samples were collected with 12 hour time resolution at both sites. Selected
28 metals, main anions, cations, and elemental and organic carbon were determined.

29 The evolution of soluble V and Ni concentrations (typical markers of heavy fuel oil
30 combustion) was related to meteorology and ship traffic intensity in the Sicily Channel,
31 using a high resolution regional model for calculation of back trajectories. Elevated
32 concentration of V and Ni at Capo Granitola and Lampedusa are found to correspond
33 with airmasses from the Sicily Channel and coincidences between trajectories and
34 positions of large ships; the vertical structure of the planetary boundary layer also
35 appears to play a role, with high V values associated with strong inversions and stable
36 boundary layer. The V concentration was generally lower at Lampedusa than at Capo
37 Granitola, where it reached a peak value of 40 ng/m³.

38 Concentrations of rare earth elements, La and Ce in particular, were used to identify
39 possible contributions from refineries, whose emissions are also characterized by
40 elevated V and Ni amounts; refinery emissions are expected to display high La/Ce and
41 La/V ratios, due to the use of La in the fluid catalytic converter systems. In general, low
42 La/Ce and La/V ratios were observed in the PM samples. The combination of the

43 analyses based on chemical markers, arimass trajectories, and ship routes allows to
44 unambiguously identify the large role of the ship source in the Sicily Channel.
45 Based on the sampled aerosols, ratios of the main aerosol species arising from ship
46 emission with respect to V were estimated with the aim of deriving a lower limit for the
47 total ship contribution to PM₁₀. The estimated minimum ship emission contributions to
48 PM₁₀ was 2.0 µg/m³ at Lampedusa, and 3.0 µg/m³ at Capo Granitola, corresponding to
49 11% and 8.6% of PM₁₀, respectively.

50
51

52 **1. Introduction**

53
54 Ship emissions may significantly affect atmospheric concentrations of several important
55 pollutants, especially in maritime and coastal areas (e.g. Endresen et al., 2003). Main
56 emitted compounds are carbon dioxide (CO₂), nitrogen oxides (NO_x), sulfur dioxide
57 (SO₂), carbon monoxide (CO), hydrocarbons, and primary and secondary particles.
58 Thus, ship emissions impact the greenhouse gas budget (Stern, 2007), acid rain
59 (through NO_x and SO₂ oxidation products; Derwent et al., 2005), human health (CO,
60 hydrocarbons, particles; Lloyd's Register Engineering Services, 1995; Corbett et al.,
61 2007) and solar radiation budget through aerosol direct and indirect effects (black
62 carbon and sulfur containing particles; Devasthale et al., 2006; Lauer et al., 2007;
63 Coakley and Walsh, 2002).

64 Heavy oil fuels used by ships contain varying transition metals. The aerosol emitted by
65 ship engines is formed at high temperature (>800°C) from V, Ni, Fe compounds
66 (Sippula et al., 2009). The thermodynamics predicts that the metals in these particles
67 are mainly present as oxides. Sulfuric acid is found to form a liquid layer on the metal
68 oxide ultrafine particles, leading to the metal partial dissolution, probably increasing the
69 toxicity of the particles when inhaled.

70 In spite of the large amount of gas and particulate emitted by ships, maritime transport
71 is relatively clean if calculated per kilogram of transported good. However, maritime
72 transport has been increasing with respect to air and road transport (Micco and Pérez,
73 2001; Grewal and Haugstetter, 2007). In addition, emissions from other transport
74 sectors are decreasing due to the implementation of advanced emission reduction
75 technologies, and the relative impact of shipping emissions is increasing.

76 Regulations aiming at reducing emissions based on restrictions on the fuel sulfur
77 content (sulfur emission control areas, SECAs) have been implemented in several
78 regions. Although the legislation is focussed on sulfur emissions, the overall health and
79 environmental effects depend in complex way on the physical and chemical properties
80 of the emissions (WHO, 2013). Several studies have been carried out to determine the
81 detailed chemical composition of shipping emissions (Agrawal et al., 2008a and b,
82 Moldanová et al., 2009, Murphy et al., 2009, Lyyräinen et al 1999, Cooper, 2003, Sippula
83 et al. 2014); however, , the ships emissions are still poorly characterized with respect to
84 on-road vehicles.

85 A large variety of anthropic sources (refineries, power plants, intense ship traffic, etc.)
86 and natural emissions make the Mediterranean region one of the most polluted in the
87 world (e.g., Kouvarakis et al., 2000; Marmar and Langmann, 2005). The multiplicity of
88 Mediterranean sources (some of which with the same markers of ship aerosol) makes
89 difficult the quantification of ship contribution to the total aerosol amount (e.g., Becagli
90 et al., 2012).

91 The contribution of ships and harbour emissions to local air quality, with specific focus
92 on atmospheric aerosol, has been investigated using models (Trozzi et al., 1995;
93 Gariazzo et al., 2007; Eyring et al., 2005; Marmar et al., 2009), experimental analyses
94 at high temporal resolution (Ault et al., 2010; Contini et al., 2011; Jonsson et al., 2011;
95 Diesch et al., 2013; Donato et al., 2014), receptor models based on the identification
96 of chemical tracers associated with ship emissions (Viana et al., 2009; Pandolfi et al.,
97 2011; Cesari et al., 2014), and integrated approaches with receptor and chemical
98 transport models (Bove et al., 2014). Few studies exist in open sea (Becagli et al.,
99 2012; Schembari et al., 2014; Bove et al., 2016).

100 In this context, studies performed at Mediterranean sites, where it is possible to
101 distinguish ship emission from other sources of heavy fuel oil combustion, are important
102 to investigate the current impact of the ship emissions on primary and secondary
103 aerosols. This study contributes to the identification and characterization of the
104 emissions from ships and the impact on the aerosol distribution in the central
105 Mediterranean. The experiment was set up with the aim of unambiguously recognizing
106 the ship source by a combination of methods.

107

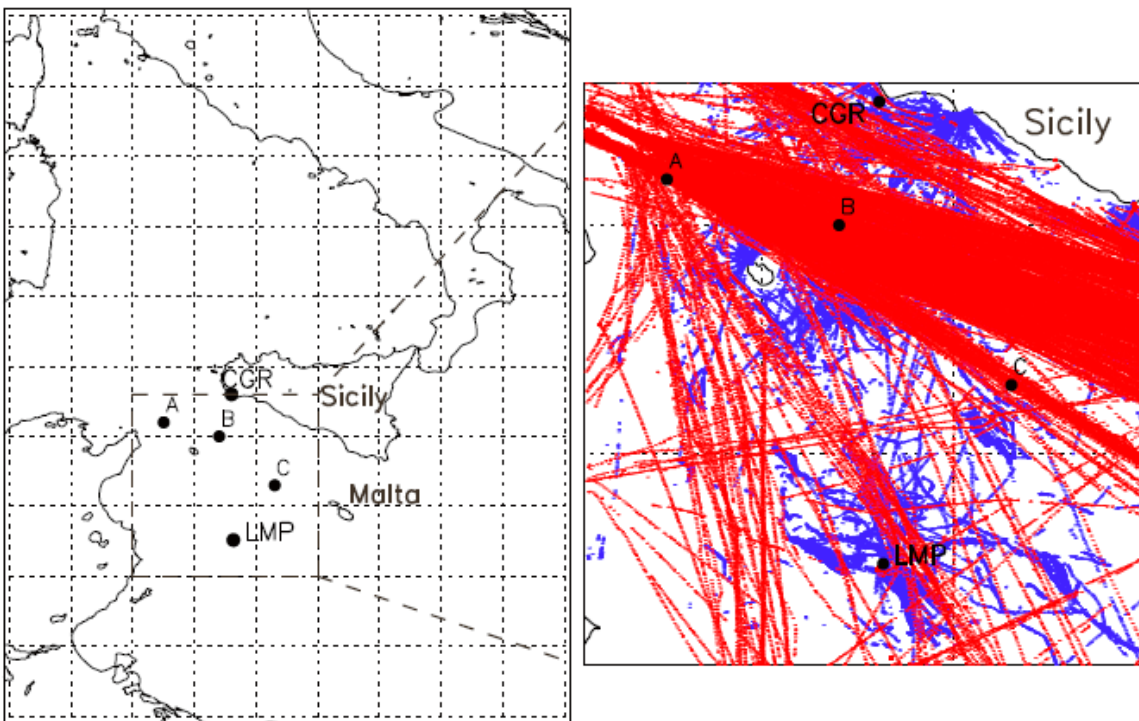
108 **2. Measurements and methods**

109

110 In a previous study (Becagli et al., 2012) we used measurements of PM₁₀ concentration
111 and chemical composition carried out at Lampedusa to investigate the role of ship
112 emissions in the central Mediterranean. Vanadium and Nickel were used as tracers of
113 heavy fuel combustion together with trajectory analyses to assess the role of ship
114 traffic. The ship source, however, could not be unequivocally separated from possible
115 influences from refineries and power plants, which use similar fuels. In summer 2013
116 we addressed the same topic by implementing a specific strategy to target the aerosols
117 due to ship emissions. PM₁₀ samples were collected in parallel at Lampedusa (LMP) and
118 at Capo Granitola (CGR), i.e., respectively South and North of the main shipping route
119 through the Mediterranean, with the aim of isolating the ship source. The chemical
120 analyses of the collected samples were complemented with measurements of Rare
121 Earth Elements (REEs), trajectories and planetary boundary layer information from a
122 high resolution regional model, and actual observations of ship traffic. The combination
123 of these approaches allows to unambiguously identify the ship source, and permits to
124 constrain its contribution to PM₁₀ in the central Mediterranean.

125 The PM₁₀ samples were collected in summer 2013 as a contribution to the Chemistry
126 and Aerosol Mediterranean Experiment (ChArMEx; <http://charmex.lscce.ispl.fr>).
127 Lampedusa is one of the supersites of the ChArMEx experiment; a list of the

128 instruments deployed during the special observing period 1a of ChArMEx, and of the
129 measurement strategy, meteorological conditions, and main observations is given by
130 Mallet et al. (2016).
131



132
133
134 Figure 1. Map of the study area with the sites of Lampedusa (LMP) and Capo Granitola
135 (CGR) (left panel). A, B, and C indicate the three sites selected to study the stability of
136 the boundary layer in the Sicily Channel (see section 3.2.2). The ship routes in the
137 study area during the first 10 days of June 2013 are displayed in the right panel. Red
138 and blue dots show the routes of merchant and fishing vessels, respectively.

139
140
141 **2.1. Aerosol sampling and chemical analyses**

142
143 PM₁₀ was sampled at two sites: at the Station for Climate Observations, maintained by
144 ENEA (the Italian Agency for New Technologies, Energy, and Sustainable Economic
145 Development) on the island of Lampedusa (35.5°N, 12.6°E), and at the Italian CNR
146 (National Research Council) Research Centre at Capo Granitola (36.6°N, 12.6° E).
147 Lampedusa is a small island in the Central Mediterranean sea, more than 100 km far
148 from the nearest Tunisian coast. At the Station for Climate Observations, which is
149 located on a 45 m a.s.l. plateau on the North-Eastern coast of Lampedusa, continuous
150 observations of aerosol properties (di Sarra et al., 2011, 2015; Becagli et al., 2013;
151 Marconi et al., 2014; Calzolari et al., 2015; Sellitto et al., 2017), aerosol radiative effects
152 (e.g., Casasanta et al., 2011; di Sarra et al., 2011; Meloni et al., 2015), and other

153 climatic parameters are carried out. Figure 1 shows the map of the central
154 Mediterranean with the measurement stations.

155 PM₁₀ is routinely sampled on a daily basis at LMP (Becagli et al., 2013; Marconi et al.,
156 2014; Calzolari et al., 2015) by using a low volume dual channel sequential sampler
157 (HYDRA FAI Instruments) equipped with two PM₁₀ sampling heads operating in accord
158 with UNI EN12341. For the intensive ChArMEx campaign, samples were collected at 12-
159 hour resolution (8:00-20:00 and 20:00-8:00 local time) from 1 June to 3 August, 2013.
160 The two channels operated in parallel and were loaded with different types of filters:
161 the first one with 47 mm diameter, 2 µm nominal porosity Teflon filters, and the second
162 one with 47 mm pre-fired, 2 µm nominal porosity, quartz filters. Ion chromatographic
163 analysis of soluble ions, atomic emission spectroscopy for soluble metals, and proton-
164 induced X-ray emission (PIXE) for the total (soluble+insoluble) elemental composition
165 were carried out on the Teflon filters. Elemental (EC) and organic carbon (OC) were
166 measured by analysing the quartz filters.

167 The sampling site at CGR is located at Torretta Granitola, a Research Center of the
168 Italian National Research Council, in South-Western Sicily (12 km from Mazara del
169 Vallo). The sampler was installed on the roof of one of the research centre buildings at
170 about 20 m a.s.l., directly on the coastline, facing the strait of Sicily.

171 At CGR PM₁₀ samples were collected at 12 hour resolution (8:00-20:00 and 20:00-8:00
172 local time) with a TECORA Skypost sequential sampler on 47 mm pre-fired 2 µm
173 nominal porosity quartz filters, which were used to determine ions, metals, EC and OC
174 on different fractions of the filter. Due to technical problems, some daytime (8:00-
175 20:00) samplings were lost at CGR.

176 The PM₁₀ mass was determined by weighting the filters before and after sampling with
177 an analytical balance in controlled conditions of temperature (20±1 °C) and relative
178 humidity (50±5 %). The estimated error on PM₁₀ mass is around 1% at 30 µg/m³ in the
179 applied sampling conditions.

180 A quarter of each Teflon filter from LMP and a 1.5 cm² punch of the quartz filter from
181 CGR were analysed by Ion Chromatography (IC) in the analytical conditions described
182 in Marconi et al. (2014). The estimated uncertainty for IC measurements is 5% for all
183 the considered ions.

184 Blank values were negligible with respect to the concentration in the samples for Teflon
185 filters. Blank values for quartz filters were negligible for most of the analyzed species.
186 For some species characterized by high blank values, always lower than the 25th
187 percentile value, they were subtracted from the measured concentrations.

188 Another quarter of the Teflon filter from LMP, and another 1.5 cm² punch of the quartz
189 filter from CGR were extracted in ultrasonic bath for 15 min with MilliQ water acidified
190 at pH 1.5–2 with ultrapure HNO₃ obtained by sub-boiling distillation. This extract was
191 used for the metals soluble part determination by means of an Inductively Coupled
192 Plasma Atomic Emission Spectrometer (ICP-AES, Varian 720-ES) equipped with an
193 ultrasonic nebulizer (U5000 AT+, Cetac Technologies Inc.). The pH chosen value is the
194 lowest found in rainwater (Li and Aneja, 1992) and leads to the determination of the

195 metals fraction available to biological organisms and, for some metals (e.g. V and Ni),
 196 related to the anthropic source (Becagli et al., 2012).

197 The remaining half Teflon filter from Lampedusa another punch of the quartz filter from
 198 CGR were used for the determination of metals by ICP-AES through the solubilisation
 199 procedure reported in the EU EN14902 (2005) rule, by using concentrated sub-boiling
 200 distilled HNO₃ and 30% ultrapure H₂O₂ in a microwave oven at 220°C for 25 min (P =
 201 55 bar). This solubilisation procedure is not able to completely dissolve the silicate
 202 species. However, this procedure allows to recover at least 70% of the same elements
 203 measured by proton induced X ray emission technique also for elements with dominant
 204 crustal source (unpublished data), due to the low crustal aerosol load in these sampling
 205 period (e.g., Mailler et al., 2016). La and Ce presented very low concentrations in the
 206 collected aerosol samples. Thus, particular attention was devoted to the minimization of
 207 the La and Ce detection limit. In the used sampling and analytical conditions of LMP
 208 samples the detection limits for La and Ce are 0.02 ng/m³ and 0.08 ng/m³, respectively,
 209 and are about 4 times higher for the CGR samples, due to the smaller filter portion used
 210 for the analysis.

211 The OC and EC measurements were carried out on a 1.5 cm² punch of the quartz filters
 212 from Lampedusa and Capo Granitola by means of a Sunset thermo-optical
 213 transmittance analyser, following the NIOSH protocol (Wu et al, 2016).

214 The overall aerosol sampling and analytical strategy for the two sites are reported in
 215 table 1.

216

217 **Table 1.** Sampling strategy and chemical measurements carried out on each filter for
 218 the two sites: Lampedusa (LMP) and Capo Granitola (CGR).

Sampling site	Filter	Sampling interval, local time.	Measurements
LMP	Teflon	8:00-20:00 (daytime sample)	<ul style="list-style-type: none"> • PM₁₀; • Ions by IC (1/4 of the filter); • metals in HNO₃ pH 1.5 room temperature extract by ICP-AES (1/4 of the filter);
		20:00-8:00 (nighttime sample)	<ul style="list-style-type: none"> • metals in HNO₃-H₂O₂ in microwave oven extract by ICP-AES (1/2 filter)
	Quartz	8:00-20:00 (daytime sample)	<ul style="list-style-type: none"> • EC/OC by thermo-optical analyser (1.5 cm x 1 cm punch)
		20:00-8:00 (nighttime)	

		sample)	
CGR	Quartz	8:00-20:00 (daytime sample)	<ul style="list-style-type: none"> • PM₁₀; • Ions by IC (1.5 cm x 1 cm punch); • metals in HNO₃ pH 1.5 room temperature extract by ICP-AES (1.5 cm x 1 cm punch);
		20:00-8:00 (nighttime sample)	<ul style="list-style-type: none"> • metals in HNO₃-H₂O₂ in microwave oven extract by ICP-AES (1.5 cm x 1 cm punch) • EC/OC by thermo-optical analyser (1.5 cm x 1 cm punch)

219
220
221
222
223

2.3. Atmospheric model and trajectory calculations

224 Numerical simulations with a non-hydrostatic mesoscale atmospheric model were used
225 to characterize the meteorological conditions in the Sicily Channel during the campaign
226 and to support the interpretation of the experimental results. The Weather Research
227 and Forecasting (WRF) model (Skamarock et al., 2008) outputs, provided by the
228 Department of Physics of the University of Genoa, Italy, were used, covering the entire
229 Mediterranean with a grid spacing of 10 km and hourly temporal resolution. Initial and
230 boundary conditions to drive WRF simulations were obtained from the Global Forecast
231 System operational global model (Environmental Modeling Center, 2003) outputs
232 (0.5x0.5 squared degrees). Some recent applications of the modelling chain are
233 described in Mentaschi et al. (2015) and Cassola et al. (2016), where full details on the
234 model configuration can also be found.

235 In particular, the WRF 3-D hourly meteorological fields were used to calculate backward
236 trajectories with the NOAA HYbrid Single-Particle Lagrangian Integrated Trajectory
237 Model (HYSPLIT; Stein et al. 2015). The trajectories were used to assess the origin of
238 the air masses impacting the monitoring sites and to support the source attribution
239 suggested by the analysis of specific markers (see Section 3.2.2). The use of a high-
240 resolution regional atmospheric model for trajectory calculations allows a better
241 representation of boundary layer properties and mesoscale phenomena such as
242 land/sea breezes, which can have a relevant impact especially in complex topography
243 coastal sites like CGR.

244 Also, the high temporal resolution of meteorological data (hourly instead of three- or
245 six-hourly products typically available from global models) permits a better description
246 of diurnal cycles as well as a more accurate trajectory computation, without time
247 interpolation between subsequent atmospheric fields (Solomos et al., 2015).

248 Specifically, 48-h long back trajectories arriving at LMP and CGR were computed from a
249 reference height of 10 m above the ground level, starting every six hours for the whole
250 period of the campaign, from 10 June to 31 July, 2013.

251
252
253
254
255
256
257
258
259
260
261
262
263
264
265
266
267
268
269
270
271
272
273
274
275
276
277
278
279
280
281
282
283
284
285
286
287
288
289
290
291
292
293

2.4. Ships/marine traffic

Position and main characteristics of the ships travelling in the central Mediterranean were derived from the MarineTraffic database (<http://www.marinetraffic.com/>), which provides data with a high temporal resolution (about 3-5 minutes) by means of the Automatic Identification System (AIS).

Three classes of ships defined by the AIS classification were considered: all the ships, the merchant (i.e. cargo and tanker), and the fishing vessels. Merchant and fishing vessels are the most frequent ships in the Sicily Channel; merchant ships are expected to produce the highest impact due to their higher emissions (http://ec.europa.eu/environment/archives/air/pdf/chapter2_ship_emissions.pdf).

3. Results

3.1. PM₁₀ chemical composition at the two sites

The sea salt aerosol (SSA) component of PM₁₀ was estimated as the sum of Na⁺, Mg²⁺, Ca²⁺, K⁺, sulfate and chloride sea salt (ss) fractions. Details on the calculation of sea salt Na⁺ and Ca²⁺, and non-sea salt (nss) fractions are reported in Marconi et al. (2014). The Mg²⁺, Ca²⁺, K⁺, and sulphate sea salt fractions were calculated from sea salt Na⁺ (ssNa⁺) by using the ratio of each component to Na⁺ in bulk sea water: Mg²⁺/Na⁺ = 0.129, Ca²⁺/Na⁺ = 0.038, K⁺/Na⁺ = 0.036, SO₄²⁻/Na⁺ = 0.253 (Bowen, 1979). Chloride undergoes depletion processes during aging of sea spray, mainly due to exchange reactions with anthropogenic H₂SO₄ and HNO₃, leading to re-emission of gaseous HCl in the atmosphere. Thus, for chloride we use the measured chloride concentration instead of the one calculated from ssNa⁺. Thus,

$$\text{SSA} = 1.46 * [\text{ssNa}^+] + [\text{Cl}^-].$$

The crustal component is calculated from Al, which represents 8.2% of the upper continental crust, UCC (Henderson and Henderson 2009). A previous study using an extensive data set at Lampedusa showed that the crustal content determined from the total Al was in very good agreement with calculations made from the sum of the metal oxides (Marconi et al., 2014). However, in this study we use measurements of the soluble Al concentration obtained by ICP-AES on the solution obtained with H₂O₂ and HNO₃ in microwave oven instead of the total Al content. Therefore, in this work we underestimate the crustal contribution by about 30% (unpublished results). However, it must be emphasized that the crustal aerosol contribution was very low throughout the measurement campaign.

Figure 2 shows the time series of the main PM₁₀ components at LMP and CGR. An intense Mistral event occurred from 22 June to 1 July. Mistral events are characterized

294 by strong winds from the north-westerly sector, and often by subsiding air masses
 295 originating from the free troposphere (Jiang et al., 2003). Thus, elevated values of SSA
 296 and low concentrations of other compounds are generally found during Mistral at
 297 Lampedusa.

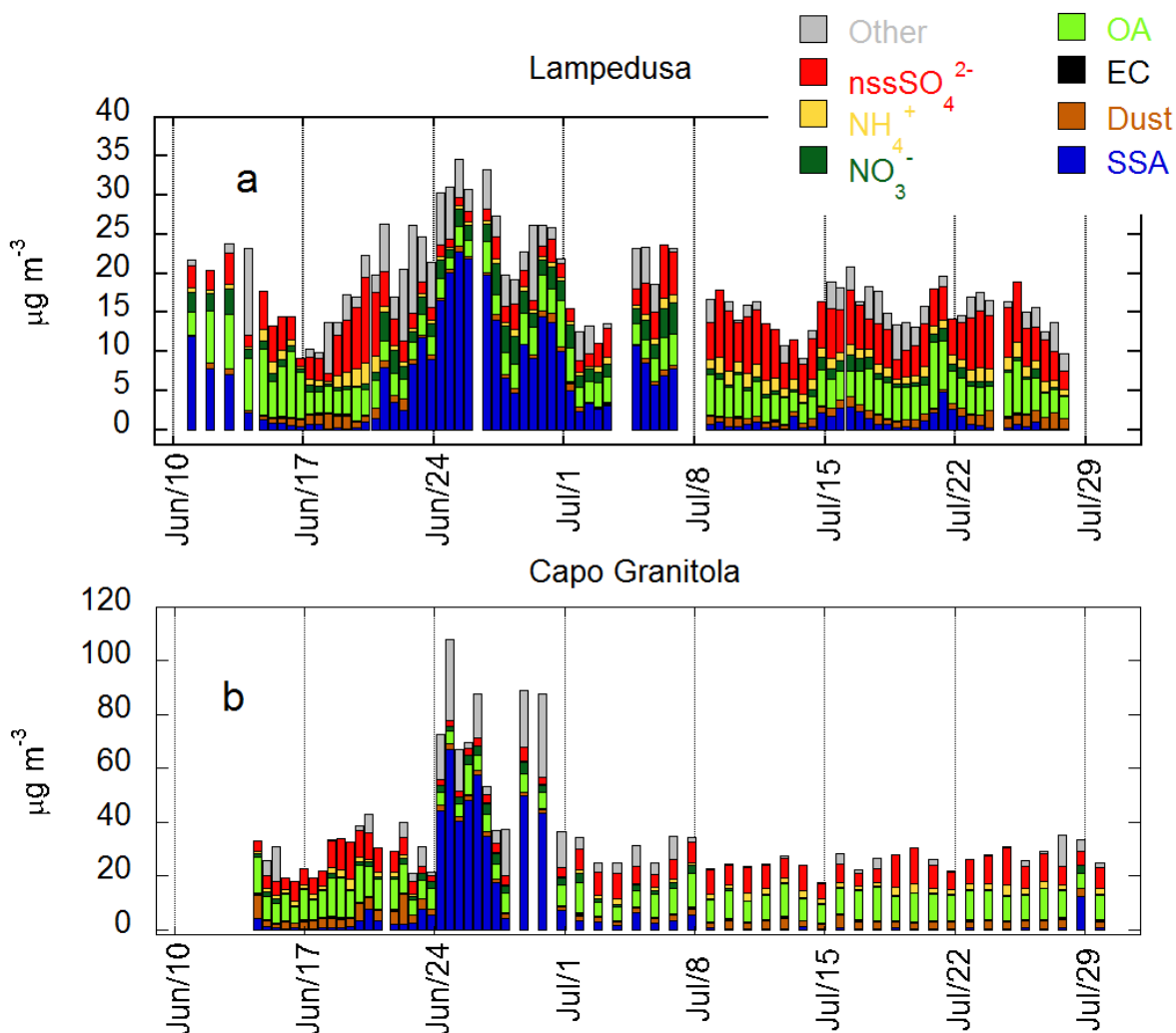
298 Average concentrations of PM₁₀ and of the different aerosol components for the whole
 299 measurement campaign and for the non-Mistral conditions are reported in Table 2. The
 300 averages were calculated over a homogeneous dataset, i.e., when measurements are
 301 available at both sites.

302
 303 **Table 2.** Mean and standard deviation of PM₁₀ load and composition, and percentage
 304 with respect to PM₁₀ (in bracket) at Lampedusa and Capo Granitola. Mean, standard
 305 deviation and percentage are calculated on homogeneous data sets for both sites
 306 considering all the common sampling ("all data" columns) and excluding the mistral
 307 events ("Mistral excluded" columns).

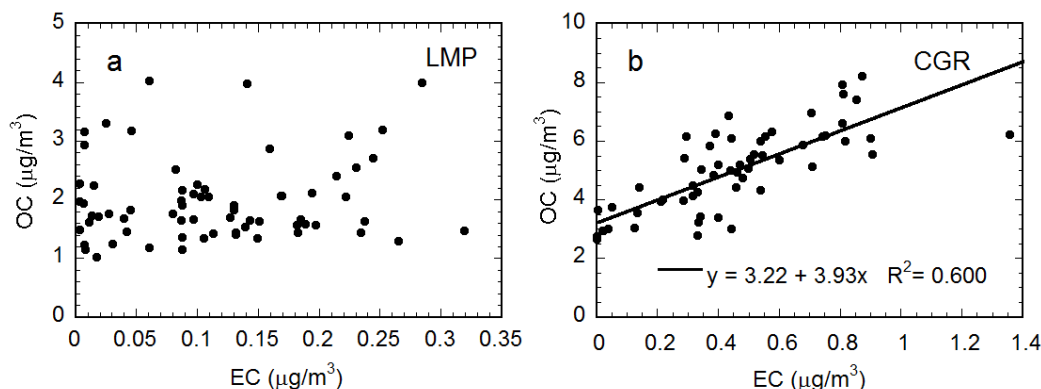
308
 309

	Lampedusa		Capo Granitola	
	All data	Mistral excluded	All data	Mistral excluded
PM₁₀ (µg/m³)	18.0±6.6	16.3±5.2	34.1±18.9	27.2±6.5
Sea Salt Aerosol (µg/m³)	4.63±6.30 (25.7%)	2.33±3.21 (14.3%)	8.14±15.50 (23.9%)	2.12±6.51 (7.8%)
Crustal Aerosol (µg/m³)	0.82±0.44 (4.6%)	0.90±0.43 (5.5%)	2.80±1.7 (8.2%)	3.02±1.75 (11.1%)
nssSO₄²⁻ (µg/m³)	3.95±2.28 (21.9%)	4.40±2.22 (27.0%)	6.78±3.08 (19.9%)	7.53±2.78 (27.7%)
NH₄⁺ (µg/m³)	0.98±0.56 (5.5%)	1.09±0.55 (6.7%)	1.48±0.94 (4.3%)	1.66±0.87 (6.1%)
NO₃⁻ (µg/m³)	1.25±1.00 (7.0%)	1.02±0.02 (6.2%)	1.35±1.11 (4.0%)	1.01±0.82 (3.7%)
Organic aerosol (µg/m³)	3.86±1.56 (21.4%)	4.04±1.59 (24.8%)	9.02±2.52 (26.5%)	9.53±2.29 (35.0%)
Elemental carbon (µg/m³)	0.15±0.08 (0.8%)	0.15±0.08 (0.9%)	0.44±0.28 (1.3%)	0.51±0.26 (1.9%)
Unknown (µg/m³)	2.52±3.26 (14.0%)	2.20±3.40 (13.5%)	4.11±7.78 (12.1%)	1.82±4.48 (6.7%)

310 The largest PM_{10} values were associated with elevated SSA during the Mistral event at
 311 both sites. PM_{10} is about two times larger at Capo Granitola than at Lampedusa. The
 312 PM_{10} measured during the campaign at Lampedusa was significantly lower than its long-
 313 term average ($31.5 \mu\text{g}/\text{m}^3$; Marconi et al., 2014). No Saharan dust transport events
 314 occurred at low altitude in this period (e.g., Mailler et al., 2015), and the crustal aerosol
 315 contribution remained very low and almost constant at both sites (average $< 1 \mu\text{g}/\text{m}^3$
 316 at LMP and around $3 \mu\text{g}/\text{m}^3$ at CGR corresponding to 4.6% and 8.2% of the PM_{10} at
 317 LMP and CGR respectively).



318
 319
 320 Figure 2. Time series of the main aerosol components at LMP (plot a) and CGR (plot b).
 321 Note the different vertical scales of the graphs. OA stands for organic aerosol.
 322
 323
 324



325
 326
 327 Figure 3. Scatter plot of OC vs. EC at LMP (plot a) and CGR (plot b). Note the different
 328 vertical scales.

329
 330
 331 SSA accounted for about 26% and 24% of PM_{10} at LMP and CGR, respectively. The SSA
 332 contribution was about 14% of PM_{10} at LMP and 8% at CGR during the periods not
 333 influenced by the Mistral. Non-sea salt SO_4^{2-} was the most abundant among the
 334 secondary inorganic species.

335 Nitrate concentrations, although relatively high at both sites, are in agreement with the
 336 long term measurements performed at Lampedusa (e.g., Calzolari et al., 2015) and with
 337 data from other remote sites in the western (Mallorca; e.g. Simo et al., 1991) and
 338 eastern Mediterranean (Finokalia; e.g. Mihalopoulos et al., 1997).

339 Organic aerosol (OA) was the most abundant component at CGR, where its mean
 340 concentration was $> 9 \mu g/m^3$ and represented 35% of PM_{10} in the days not
 341 characterized by Mistral.

342 Elemental carbon and organic carbon show higher values at CGR than LMP. At CGR
 343 moderate and elevated values of OC and EC appear correlated ($R^2=0.60$; $n = 59$; Figure
 344 3b), suggesting a strong influence from carbon species primary sources, characterized
 345 by the simultaneous EC and OC emission. The influence from primary sources is
 346 apparent at $EC > 0.4 \mu g/m^3$. At LMP, on the contrary, OC was not correlated with EC
 347 (figure 3a), indicating a strong impact of OC secondary and/or natural sources. This
 348 confirms that Lampedusa may be considered a background site in the central
 349 Mediterranean (see e.g., Artuso et al., 2009; Henne et al., 2010), and the observations
 350 there may be taken as representative for a relatively wide open sea region.

351 Thus, we used a conversion factor of 1.8 (typical for urban background sites, Turpin
 352 and Lin, 2001) at CGR, and of 2.1 (typical for remote sites characterized by high impact
 353 of secondary sources, Turpin and Lin, 2001) at LMP to estimate the total organic
 354 aerosol amount from the OC measured values. Once estimated OA with this method,
 355 the sum of the various species accounted to more than 85% of the measured mass at

356 both sites. The unreconstructed mass could be due to an underestimation of OA from
 357 OC, or to the presence of bound water not removed by the desiccation procedure at
 358 50% relative humidity (Tsyro, 2005; Canepari et al., 2013).

359
 360

361 **3.1.1. Ship emission markers: V and Ni**

362

363 Several studies focussed on the identification of shipping emissions specific tracers
 364 (Viana et al., 2008; Becagli et al., 2012, Isakson et al., 2001, Hellebust et al., 2010).
 365 Vanadium and Nickel are generally considered the best markers for this source because,
 366 after sulfur, they are the main impurities in heavy fuel oil (Agrawal et al., 2008a and b).
 367 The soluble fraction of these metals is even more representative for the ship source
 368 (Becagli et al., 2012).

369 Following Becagli et al. (2012), we used measurements of the V and Ni soluble fractions
 370 (V_{sol} and Ni_{sol} , respectively). In the data set here considered the V_{sol} and Ni_{sol} ratio with
 371 respect to Al were always more than 10 times larger than for UCC, as expected for
 372 cases dominated by heavy oil combustions sources (ships, refineries, power plants,
 373 stainless steel production plants).

374 Table 3 reports slope, correlation coefficient, and number of samples of the linear
 375 correlation between V_{sol} and Ni_{sol} .

376

377

378 **Table 3.** Correlation parameters between V and Ni at LMP and CGR PM_{10} samples for
 379 all the samples and for samples with V concentration higher than 6 ng/m^3 .

380

		Slope (\pm uncertainty)	R²	n.
LMP	All data	2.94 \pm 0.03	0.986	124
	$V_{sol} > 6\text{ ng/m}^3$	2.99 \pm 0.03	0.994	44
CGR	All data	2.82 \pm 0.08	0.950	59
	$V_{sol} > 6\text{ ng/m}^3$	3.00 \pm 0.05	0.989	34

381

382

383 V_{sol} and Ni_{sol} are highly correlated, suggesting a common source. The obtained slope of
 384 the regression line (2.8-2.9, that increases to 3.0 for samples with $V_{sol} > 6\text{ ng/m}^3$) is in
 385 the range of ratios typical for heavy fuel oil combustion sources. The same value was
 386 found at Lampedusa by Becagli et al. (2012), considering data from 2004 to 2008. The
 387 behaviour of V, Ni, and their ratio are then representative of heavy fuel oil combustion.
 388 It must be emphasized that the V/Ni ratio is expected to display a large variability due
 389 to varying fuel composition and engine operating conditions (Mazzei et al., 2008;
 390 Agrawal et al., 2008a and b, Viana et al. 2009; Pandolfi et al., 2011). It is however
 391 difficult to distinguish V and Ni originating from power plants, refineries, or ship

392 engines. Moreover, several refineries are present in Sicily (Siracusa, Gela, Milazzo) and
393 in Sardinia (Cagliari) and may potentially influence the sampling sites.

394 A combination of methods is thus used in this study to unequivocally identify the ship
395 source. The analysis is based on: additional chemical tracers, like the Rare Earth
396 Elements, whose behaviour is specific for the refinery and the ship sources; high
397 resolution back-trajectories, based on data from the high resolution regional model;
398 information on the vertical mixing in the atmospheric boundary layer; coincidences
399 between the high resolution back-trajectories and the position of different types of
400 ships in the Sicily Channel.

401

402

403 **3.1.2. Rare Earth elements**

404

405 As discussed above, anthropogenic V and Ni originate from heavy oil combustion, and
406 may be considered markers of the ship source only when other sources can be
407 excluded. Few studies propose the use of lanthanoid elements (La to Lu) to distinguish
408 refinery from ship emissions (Moreno et al., 2008a and b; Du and Turner, 2015;
409 Kulkarni et al., 2006).

410 In particular, the ratio between the La and Ce concentrations (La/Ce ratio, hereafter
411 LCR) and between La and V (hereafter LVR) can be used to identify specific sources.

412 Shipping emissions are characterised by values of LCR between 0.6 and 0.8 and LVR <
413 0.1 (Moreno et al., 2008a, 2008b).

414 Crustal aerosols are characterized by LCR ranging from 0.4 to 0.6 and LVR usually in
415 the range 0.2-0.3 (Moreno et al., 2008 a and b). LCR depends weakly on differences in
416 dust source area and collected aerosol size fraction, contrarily to LVR, which reaches
417 0.9 for large (>10 μm) particles from specific areas of Sahara (e.g., Hoggar Massif;
418 Handerson and Handerson, 2009; Moreno et al., 2006; Castillo et al, 2008).

419 Elevated values of LCR (from 1 to 13) are associated with emissions from refineries
420 (Moreno et al., 2008a; Du and Turner, 2015). This is because zeolitic fluidised-bed
421 catalytic cracking (FCC) unit enriched in La are used to crack long-chain olefins in crude
422 oil to shorter-chain products (Bozlaker et al., 2016; Du and Turner 2015; Kulkani et al
423 2006; Moreno et al., 2008a, 2008b).

424 Mixing of aerosol from different sources may produce a large variability of LCR, with
425 larger values corresponding to a stronger impact from refineries.

426 The time series of LCR and LVR at LMP and CGR is displayed in figure 4. The range of
427 values expected for crustal aerosol is highlighted in the figure. Please, note that the
428 uncertainty on LCR is very large when La and Ce concentrations are close to the
429 measurement detection limit. These cases may produce very large values of LCR which
430 are not significant; these cases were removed from the time series.

431 LCR at LMP and CGR was generally around the value expected for crustal aerosol
432 (dashed grey area in figure 4); 10 samples from LMP and 2 samples from CGR show
433 values LCR higher than 1. LCR is >1.5 in a single case, at LMP. This suggests that the
434 refineries impact is small in the collected samples.

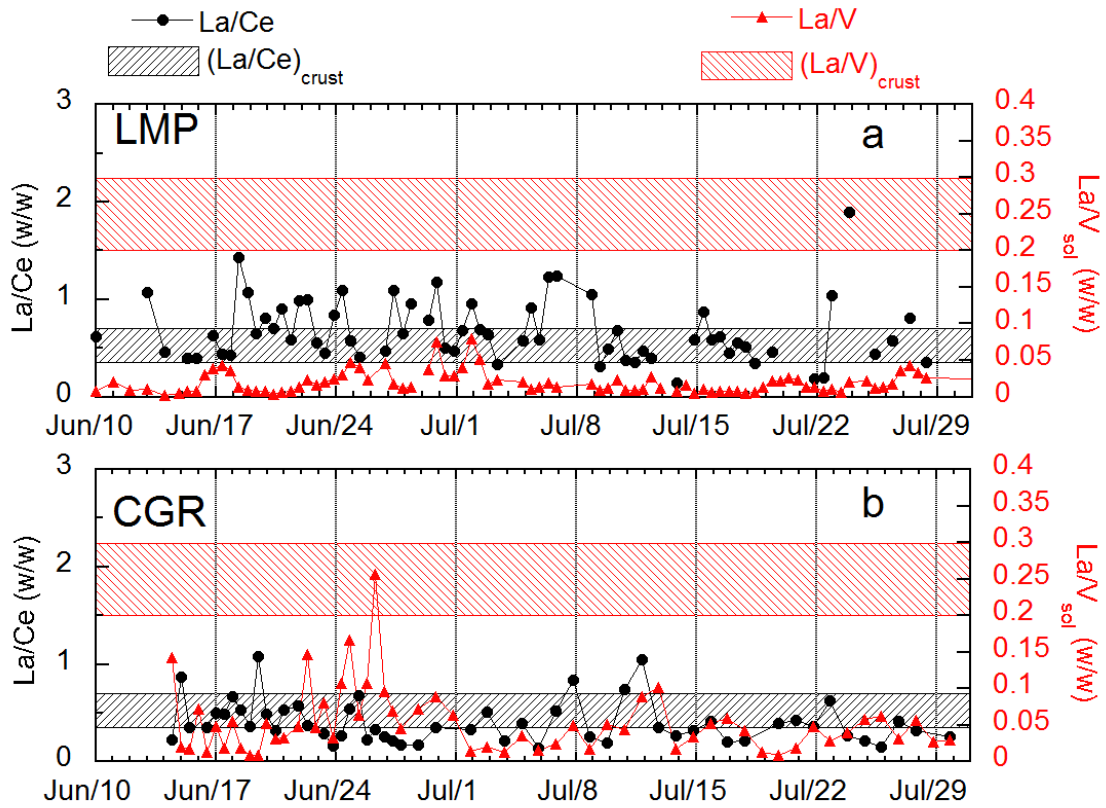
435 Moreno et al. (2008b) have shown that it is possible to identify aerosol from refineries
436 based on V, La, Ce three-component plot. This type of plot is shown in figure 5 for the
437 data from LMP and CGR. La and Ce were scaled in order to have the typical UCC
438 composition in the centre of the plot.

439 The compositions of UCC (Henderson and Henderson, 2009), African desert dust
440 (Castillo et al., 2008; Moreno et al., 2006), FCC (Kulkarni et al., 2006), La-contaminated
441 (refinery) Asian dust collected at Mauna Loa, Hawai'i (Olmez and Gordon, 1985), and
442 PM₁₀ and PM_{2.5} collected at Puertollano (Spain) in days possibly affected by refinery
443 emissions (Moreno et al., 2008b) are also displayed in figure 5.

444 The data from CGR and LMP are grouped in a region with elevated values of V, and La
445 and Ce generally lower than for refinery and dust cases.

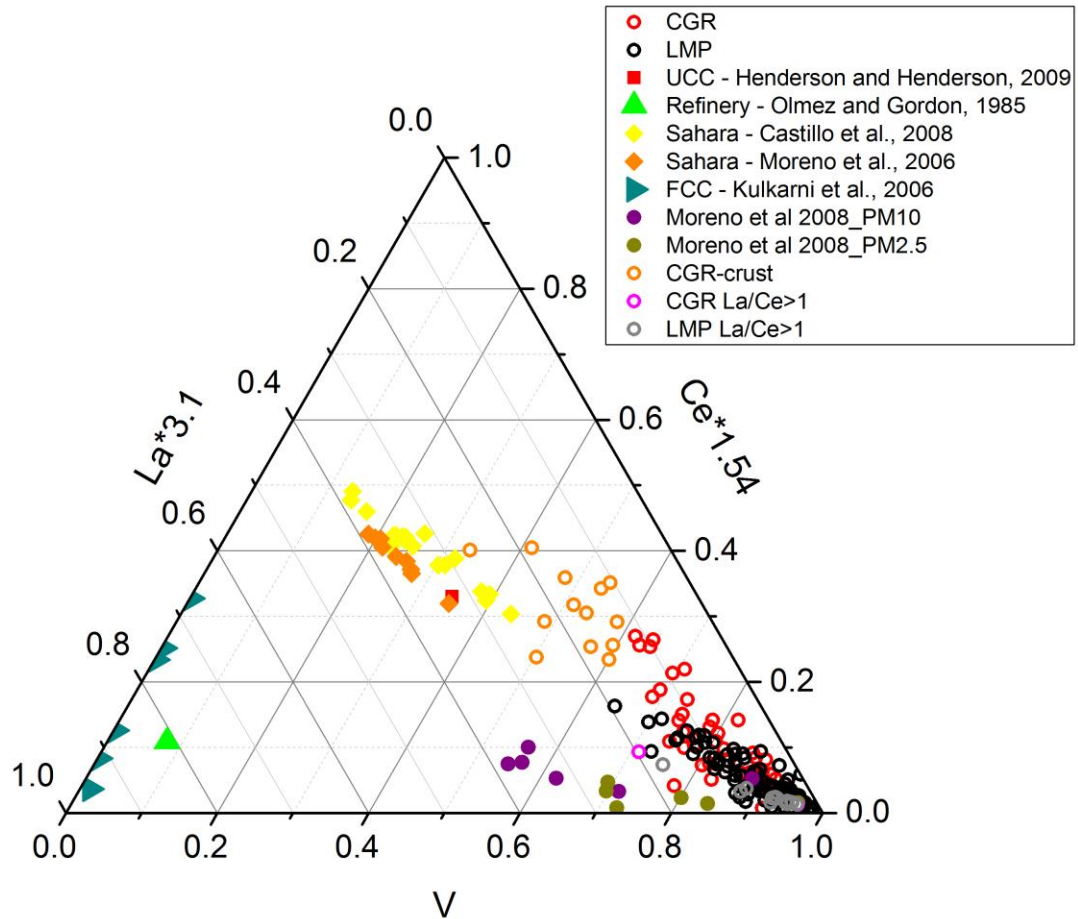
446 Data from Puertollano shown in figure 5 are relative to days characterized by winds
447 originating from sectors where refineries are located; however, these samples are
448 affected by a mix of particles from several sources, including refineries. Aerosol samples
449 from Spain affected in most cases display larger La to Ce and La to V ratios than those
450 found at LMP and CGR. The composition of all samples collected in this period at LMP is
451 consistent with a large impact from ship emissions. Some cases at CGR may suggest
452 the simultaneous occurrence of crustal and ship aerosols, or dominant crustal
453 component (orange open dots in figure 5). Therefore, these cases display a relatively
454 low V concentration and are mainly associated with the Mistral event. A limited crustal
455 contamination may possibly occur at CGR in these cases, due to resuspension due to
456 the strong wind.

457 Cases with LCR>1 (grey and pink open circle for CGR and LMP respectively) are
458 highlighted in figure 5. The aerosol composition is however consistent with the ship
459 source also in these cases, suggesting that the impact of refineries is limited.



460
 461
 462
 463
 464
 465

Figure 4. Time series of LCR and LVR at a), Lampedusa, and b), Capo Granitola. The horizontal red and grey shadow areas in each plot represent the ranges of values for upper continental crust LVR and LCR, respectively.



466 Figure 5. Three-component Ce-La-V plots for LMP and CGR. Literature data for different
 467 aerosol types are also shown.
 468

469
 470
 471

472 3.2. Trajectories and ship traffic

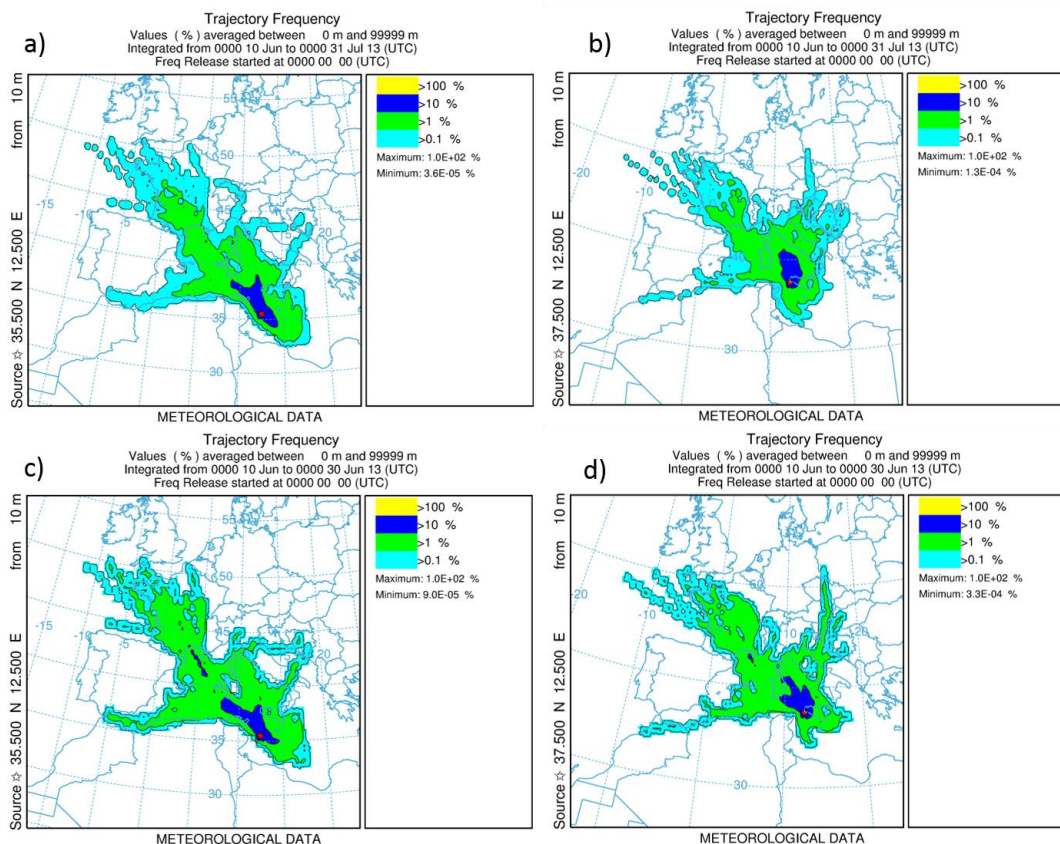
473

474 3.2.1 Origin of air masses during the campaign

475

476 All the trajectories arriving at LMP and CGR, calculated with the HYSPLIT model driven
 477 by WRF meteorological fields (see Section 2.3), are shown in an aggregated way in
 478 Figure 6, where the trajectory frequency at each point of the computing grid is shown
 479 for the whole period (upper panels) and for the 10 – 30 June interval (lower panels).
 480 The trajectory frequency pattern is elongated in the NW-SE direction at LMP, while it is
 481 distributed over a wider range of directions at CGR, despite a general prevalence of
 482 northerly sectors. The predominance of air masses coming from the northwest is
 483 particularly evident in June (lower panels); when areas with trajectory frequencies
 484 exceeding 10% are found farther to the north, up to the Gulf of Lion.

485 During the first part of the campaign (June 2013) the synoptic situation was
 486 characterized by a "dipolar" sea level pressure anomaly pattern, with positive anomalies
 487 in the western Mediterranean and negative ones in the eastern part of the basin
 488 (Denjean et al., 2016). This situation induced stronger and more frequent than usual
 489 north-westerly winds (i.e. Mistral episodes, see Section 3.1) over the Sardinia and Sicily
 490 Channels.
 491



492
 493 Figure 6. Trajectory frequency data computed at each grid cell with starting points at LMP
 494 (panels a, c) and CGR (b, d). Upper panels show values averaged over the whole period
 495 of the campaign (10 June – 31 July 2013), while lower panels are relative to the 10-30
 496 June interval.

497
 498
 499 **3.2.2 Ship traffic**

500
 501 To further investigate the mechanisms determining the presence of ship emissions
 502 markers at the two sites we investigated the relationships among the amount of V, the
 503 back-trajectory pattern, the effective number of ships influencing the air mass, the
 504 stability of the boundary layer in the ship source region (i.e., the Sicily Channel), and
 505 the REE to V ratios discussed in section 3.1.2.

506 All back-trajectories arriving at LMP and CGR were considered and all trajectory-ship
507 coincidences occurring within the last 36 hours before sampling were taken into
508 account.

509 It was assumed that the ship plume influenced the sampled air mass if:

510 - the trajectory passed within 15 km of the position of a ship

511 - the corresponding air mass altitude was less than 500 m.

512 The total number of ships fulfilling these criteria was associated with each trajectory.
513 The analysis was based on the available 1-hour time resolution meteorological fields (a
514 ship influencing a trajectory was counted once every hour).

515 To further explore the impact of different types of ships, the analysis was carried out
516 considering the following three ship categories: all the ships, the merchant (i.e. cargo
517 and tanker), and the fishing vessels.

518 The atmospheric stability is also expected to play a large role in modulating the ship
519 impact (see e.g., its influence on V amounts, Becagli et al. 2012). A temperature
520 inversion, TI, index, was calculated based on the 3D atmospheric fields of the WRF
521 model at three sites in the Sicily Channel. The temperature inversions were used as a
522 proxy to identify periods characterized by a stable boundary layer. The three sites, A
523 (37.2°N, 11.5°E), B (37.0°N, 12.4°E), and C (36.3°N, 13.3°E) (figure 1) were selected
524 in the regions of most frequent ship passage and crossing with the trajectories from
525 LMP and CGR. The TI index was calculated as the difference between the temperature
526 at the altitude of the maximum T, and at the surface. A positive TI indicates an
527 inversion, and the TI value provides an indication of the inversion strength. Only
528 positive values are considered in this analysis.

529 Figure 7 summarizes the results of this analysis. It shows the time series of the number
530 of the ships influencing the trajectories arriving at LMP and CGR, respectively, and the
531 corresponding measured values of V. Samples which show a limited influence from ship
532 emissions, determined on the basis of the La-Ce-V composition (see section 3.1.2), are
533 highlighted with arrows (orange arrows for samples with La-Ce-V ratios typical for
534 crust; pink and gray for sample possibly influenced by refineries, i.e., with LCR>1).
535 Results are shown for the three classes of ships. The positive values of TI are also
536 shown.

537 In general, there is a rather good correspondence between the cases classified as
538 influenced by ships emissions and the number of ships encountered along the
539 associated air mass trajectory at CGR. The correspondence is somewhat less evident at
540 LMP. As discussed above, the V concentration ascribed to ships (data points without
541 arrows in figure 7) is generally higher at CGR than at LMP. Part of this difference may
542 be ascribed to the shorter distance between CGR and the main shipping route crossing
543 the Sicily Channel with respect to Lampedusa, the consequent larger number of
544 encountered ships, and an aerosol dilution effect during transport from the sources to
545 LMP.

546 Maxima of V attributed to ships occurred between 19 and 20 June at CGR (about 42
547 ng/m³), and on 21 June at LMP (36.1 ng/m³). Similar concentrations were measured at
548 CGR also around 18-19 July, in conjunction with an increase in the number of merchant

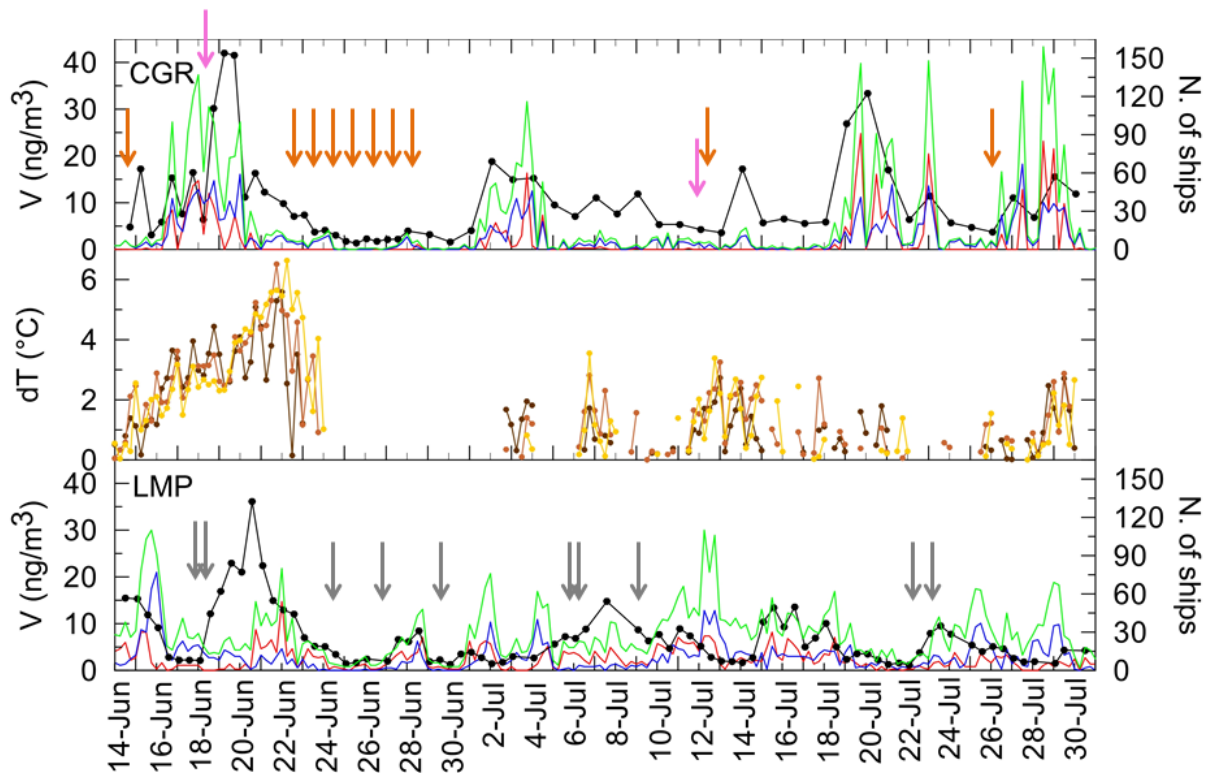
549 vessels. The 18-21 June period is the only event with high V concentrations quasi
550 simultaneously at both sites. This is due to the peculiar circulation patterns, with
551 air mass trajectories from the marine sector South of Sicily to CGR, and from the Sicily
552 channel to LMP, particularly on 18 and 19 June. The 19-21 June episode is the largest
553 occurring at LMP, both for duration and V concentration. Especially at the beginning of
554 the event, large values of V do not correspond with an increase of the number of ships
555 along the air mass trajectories.

556 A possible explanation for this behaviour is provided by the temporal evolution of TI in
557 the Sicily Channel. The temperature inversion started to develop on 14 June, and
558 gradually increased in intensity until 22 June; the TI persistence and progressive
559 increase in intensity provided suitable conditions for the ship plumes trapping in the
560 boundary layer, with a consequent build-up of the ship aerosol and V concentration.
561 This process appears particularly efficient at CGR between 21 and 25 June.

562 A similar combined dependency on number of ships and TI appears also at LMP around
563 7 July. It is interesting to note that V from ships seems to depend more directly on the
564 number of merchant ships (see, e.g., the lack of V peaks on 17 June, 12 and 29 July at
565 LMP, when the number of fishing vessels was high and the number of merchant ships
566 was low) than on the total or the fishing ships.

567 Thus, the trajectory analysis carried out in combination with the available information
568 on the ship tracks confirms that the ship emissions are the main responsible for most of
569 the moderate and elevated values of V measured at LMP and CGR during the campaign,
570 and in particular for those cases with La and Ce compatible with the ship source. This
571 analysis also clearly suggests that the boundary layer structure plays a very important
572 role in determining the impact produced by the emissions. This simplified approach
573 confirms the importance to carefully characterize the emission scenario and the
574 meteorological conditions in studies on the ships emissions impact on air quality.

575



576
 577 Figure 7. Time series of Vanadium concentration (black line with dots) and number of
 578 ships affecting the air masses sampled at CGR (upper panel) and LMP (lower panel).
 579 Green, red, and blue lines indicate respectively the total number of ships, the number of
 580 merchant (i.e. cargo and tanker), and of fishing vessels. The time evolution of the
 581 temperature inversion index (dT in the figure) at three different locations in the Sicily
 582 Channels is shown in the middle panel; brown, red, and yellow curves show the
 583 behaviour at sites A, B, and C (see text). The orange arrows identify samples classified
 584 as crustal based on the La-Ce-V concentration; pink and gray identify samples with
 585 $LCR > 1$, possibly influenced by refineries.

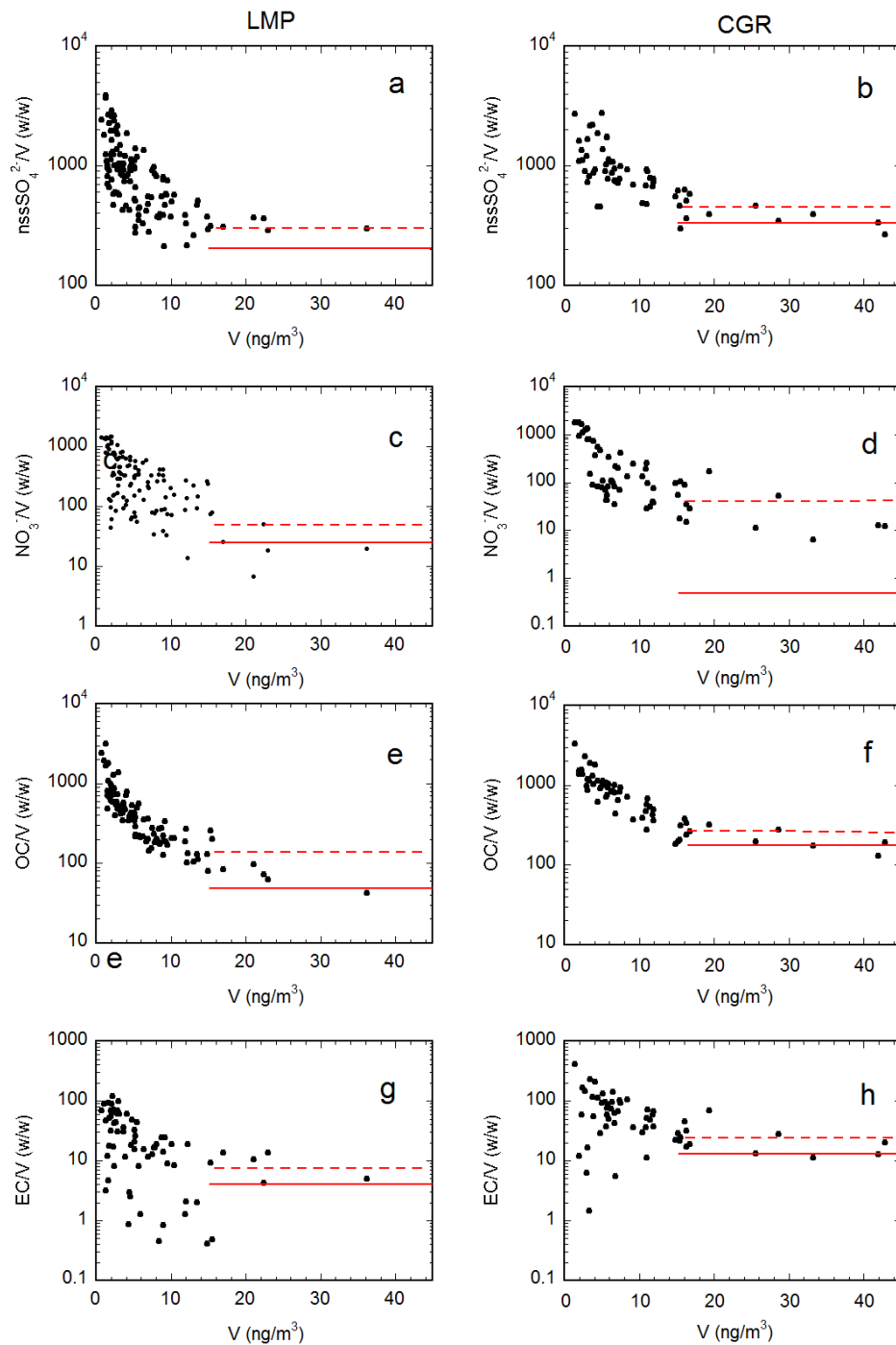
586
 587
 588

589 3.3. Sulfate, nitrate, and organic carbon from ships

590
 591 SO_2 is one of the main species emitted in the ship plume in the gas phase (Agrawal et
 592 al., 2008a, b). SO_2 is produced through oxidation of the S contained as impurity in
 593 heavy fuel oil, and is an aerosol precursor.

594 A previous study based on 5 years of data from Lampedusa (Becagli et al., 2012) has
 595 shown that the non-sea salt sulfate behaviour is not directly correlated with V and Ni

596 because several other SO_4^{2-} sources (anthropogenic, marine biogenic, crustal, volcanic)
597 contribute to the non-sea salt sulfate in the Central Mediterranean Sea.
598 The same study suggested a lower limit of about 200 for the nssSO_4^{2-}/V ratio for
599 particles originating from heavy oil combustion at Lampedusa.
600 Figure 8 shows nssSO_4^{2-}/V versus V at LMP and CGR. At both sites nssSO_4^{2-}/V decreases
601 for increasing V and reaches a lower limit at elevated values of V ($> 15 \text{ ng/m}^3$). The
602 analysis on REE, trajectories and ship traffic has shown that all samples with $V > 15$
603 ng/m^3 are strongly influenced by ships, and we assume that the ship emission is the
604 dominant source of the sampled particles for these cases. This implies that in these
605 cases virtually all sulfate originated from the ship source, and the observed lower limit
606 for nssSO_4^{2-}/V can be considered the lower limit for the sulfate to V ratio in the ship
607 plume. Thus, to derive a lower limit for this ratio we calculate the mean and standard
608 deviation of nssSO_4^{2-}/V for $V > 15 \text{ ng/m}^3$. The mean ratio and the mean ratio minus
609 one standard deviation are shown in figure 8.
610 The nssSO_4^{2-} to V ratio may still be decreasing for V around 15 ng/m^3 , and we used a
611 limit value equal to the average minus one standard deviation (dashed red lines in
612 figure 8) to estimate the minimum expected contribution from ships to the total sulfate
613 amount.
614 The calculated lower limit of the sulfate to V ratio at LMP is 207, in agreement with the
615 values of 200 estimated by Becagli et al. (2012). The nssSO_4^{2-}/V limit value at CGR,
616 323, is larger than at LMP. This difference is may be due to the contribution of other
617 sulfate sources which may contribute to the nssSO_4^{2-} even at high V concentration, and
618 to the smaller distance from the ship source with respect to LMP. This result highlights
619 the importance of remote sites like LMP to obtain information on the open
620 Mediterranean.
621



622
 623
 624
 625
 626
 627

Figure 8. Scatter plots of nssSO_4^{2-}/V (a and b), NO_3^-/V (c and d), OC/V (e and f) and EC/V (g and h) vs. V concentration at LMP (plots on the left) and CGR (plots on the right). The red lines in the plots represent the average (dashed line) and the average minus one standard deviation (solid line) calculated for samples with $V > 15 \text{ ng/m}^3$.

628 NO_x are among the main compounds emitted in the gas phase acting as aerosol
629 precursors. The photochemistry of NO_x leading to NO₃⁻ formation in the particulate
630 phase is complex, especially in summer due to the presence of high amounts of OH
631 radical (see e.g., Chen et al., 2005), and the NO_x contribution to the particulate phase
632 is not easy to be quantified.

633 Here we try to use the same approach used for sulfate for the determination of a lower
634 limit for the NO₃⁻/V ratio in the ship plume.

635 Figure 8 (plot c and d) shows the NO₃⁻/V ratio versus V at the two sites. Similarly to
636 sulfate, the average value of NO₃⁻/V for V > 15 ng/m³ is larger at CGR than at LMP.
637 However, the standard deviation at CGR is significantly larger at CGR. The NO_x
638 concentration in the ship plume close to the source is larger than that of SO₂ and is
639 strongly dependent on the engine operating conditions (Agrawal et al 2008b). The NO_x
640 lifetime is extremely low (1.8 hours during daytime and 6.5 hour during nighttime, Chen
641 et al., 2005). However, the NO₃⁻/V limit ratio values is low compared to the limit ratio
642 for SO₄²⁻. It has to be considered that NO₃⁻ takes part in other photochemical
643 atmospheric reactions that lead to its removal. In addition, the presence of HNO₃ in gas
644 phase not neutralized by NH₃ or by sea salt could explain the low NO₃⁻/nssSO₄²⁻ ratio in
645 the aerosol. Indeed, the NO₃⁻ concentration measured at LMP and CGR is 4-6 times
646 lower than that of nssSO₄²⁻ (table 1). Low amounts of NO₃⁻ with respect to SO₄²⁻ from
647 ship emissions are found in model simulations in Southern California (Dabdub, 2008).
648 Indeed, Dabdub (2008) shows that the aerosol contribution from ship emissions is
649 0.05% for NO₃⁻, and 44% for SO₄²⁻.

650 Elemental and Organic Carbon are also present in the ship plume (Shah et al., 2004). In
651 particular, OC constitutes about 15-25% and EC is generally lower than 1% of the PM
652 sampled at the plume of main ship engine powered by heavy fuel oil (Agrawal et al.,
653 2008b).

654 Figure 8 shows EC/V and OC/V versus V at LMP and CGR. Similarly to sulfate and
655 nitrate, OC/V decreases with increasing V and reaches a minimum value for V > 15
656 ng/m³ (43.1 and 179 at LMP and CGR, respectively) As discussed in section 3.1, other
657 OC sources in addition to ships are present at CGR even at high values of V.

658 The pattern of the ratio EC/V versus V is less clear; in particular, several very low values
659 of EC/V appear also at small values of V. This result is unexpected because V and EC
660 are both markers of the primary ship aerosol, but the data here presented seem to
661 suggest that non negligible EC contributions from other sources were present at CGR
662 and that different fractionating effects acted during the transport. Also in this case the
663 limit value is lower at LMP than at CGR.

664 Finally, as the limit ratios at CGR are likely affected by other sources than ship, we
665 assume that the limit ratios obtained at Lampedusa for V>15 ng/m³ are more
666 representative of cases dominated by ship emissions during summer in a wide region.
667 For this reason, the retrieved lower limits at LMP are used to quantify the ship
668 contribution also at CGR.

669
670

3.4 Contribution of the ship aerosol to PM₁₀

671
672
673
674
675
676
677
678
679
680
681
682
683
684
685
686
687
688
689
690
691
692
693
694
695
696
697
698
699
700
701
702
703
704
705
706
707
708
709
710
711
712
713

With all the limitations above described, by using the lower limits for the ratios (nssSO_4^{2-}/V), (NO_3^-/V), and (OC/V) representative for ship aerosol it is possible to estimate the minimum contribution of nssSO_4^{2-} , NO_3^- and OC emitted by ships to the total budget of these components, and also to the total PM₁₀ mass. It has to be noticed that the aerosol quantification obtained by this method is a rough estimate useful to constrain the ship aerosol contribution. In addition, due to possibly different meteorological conditions and photochemical activity, these values may vary spatially and seasonally.

The minimum ratio of each specie with respect to V, the minimum estimated contribution of ship emissions, for the average amount and for the maxima, to the total concentration of these species and to PM₁₀, are reported in Table 4. As previously discussed, the measured OC contribution is multiplied by 2.1 at LMP and by 1.8 at CGR to obtain the total organic aerosol contribution.

The estimated minimum concentration of non-sea-salt sulfate from ship emissions was $1.35 \mu\text{g}/\text{m}^3$ on average during this campaign at LMP. This value is lower than in the previous study by Becagli et al. (2012) obtained over a longer period (2004-2008). The relative contribution to the total sulfate is however similar here and in Becagli et al. (2012), suggesting a similar role of nssSO_4^{2-} from ship emissions to the total nssSO_4^{2-} budget. The study by Becagli et al. (2012) covered an extended time period (2004-2008); the consistency with that study suggests that the results obtained during ChArMEx are not specific of summer 2013, but are representative for a wider temporal and spatial range.

At CGR the minimum ship contribution to sulfate, averaged over the same time period, is higher than at LMP ($2.1 \mu\text{g}/\text{m}^3$), but this higher value corresponds to a lower contribution to the total nssSO_4^{2-} , confirming that other nssSO_4^{2-} sources are important at CGR.

Marmer and Langmann (2005) estimate that ship emissions contribute by 50% to the total amount of nssSO_4^{2-} in the Mediterranean. This value is, as expected, larger than the estimated minimum contribution we derive (about 30%).

The estimated minimum contribution by ships to the total nssSO_4^{2-} for cases with the largest ship impact (i.e. highest V concentration) is 69% and 77% at LMP and CGR, respectively.

Ships appear to contribute by small fractions to the total budget of NO_3^- . As previously mentioned, the NO_3^- atmospheric chemistry is complex and the contribution of nitrate from ship emission could be highly variable, especially in the Mediterranean region where high amount of UV radiation and highly reactive radical species are present.

Organic aerosol from ships also contributes significantly to the total OA amount and to the total PM; in particular, at LMP virtually all the OA present in cases with maximum ship impact may be attributed to the ship source.

By summing these three contributions, it is possible to estimate the total aerosol mass due to ship emissions, and its contribution to the total mass of PM₁₀. The lower limit for

714 the ship contribution was $2.0 \mu\text{g}/\text{m}^3$ and $3.0 \mu\text{g}/\text{m}^3$, corresponding to 11% and 8.6% of
 715 PM_{10} at LMP and CGR, respectively.

716
717

718 **Table 4.** Estimates of the average and maximum of the lower limit of nssSO_4^{2-} , NO_3^- ,
 719 OA, and PM_{10} from ships. Concentrations and percent with respect to the total amount
 720 of each species are reported. The maxima are derived by selecting cases with the
 721 largest ship impact (i.e. highest V concentration).

722

	nssSO_4^{2-}		NO_3^-		OA		PM_{10}	
	$(\text{nssSO}_4^{2-}/V)_{\min}=207$		$(\text{NO}_3^-/V)_{\min}=12.5$		$(\text{OC}/V)_{\min}=43.1$			
	LMP	CGR	LMP	CGR	LMP	CGR	LMP	CGR
Average contribution $\mu\text{g}/\text{m}^3$ (%)	1.35 (34%)	2.1 (31%)	0.082 (4.5%)	0.13 (9.0%)	0.59 (15%)	0.78 (8.7%)	2.0 (11%)	3.0 (8.6%)
Maximum contribution $\mu\text{g}/\text{m}^3$ (%)	7.5 (69%)	8.8 (77%)	0.45 (62%)	0.53 (100%)	3.3 (99%)	3.3 (22%)	11.2 (50%)	12.7 (42%)

723
724

725 These percent contributions are higher than the annual average for the Mediterranean
 726 Region estimated by Viana et al. (2014). It has to be considered that these authors
 727 used data from harbour or coastal sites, which are highly affected by other sources in
 728 addition to ships, and where gas-to-particle conversion is still at its initial phase.
 729 Moreover, the percentages reported in this study are relative to the summer season,
 730 when the ship contribution in the Mediterranean region is highest (Becagli et al., 2012).
 731 The estimated lower limit for the ship contribution in cases with maximum ship impact
 732 was between 42% and 50% of the total PM_{10} .

733
734

735 **Summary and conclusions**

736

737 In this study we investigate the impact of the ship emissions to PM_{10} on measurements
 738 made at two sites in the central Mediterranean. The main objectives of the study were
 739 to unambiguously identify the tracers of ship emissions in the sampled aerosol, and to
 740 obtain a lower limit for the produced impact.

741 The PM_{10} samples were collected in summer 2013, as a contribution to the Chemistry
 742 and Aerosol Mediterranean Experiment, in parallel at Lampedusa and at Capo Granitola,
 743 respectively South and North of the main shipping route through the Mediterranean.

744 The identification of aerosol originating from ships was based on an integrated analysis
 745 combining chemical analyses, calculations of backward trajectories using a high

746 resolution regional model, and on tracking of ship traffic in the Mediterranean through
747 the Automatic Identification System.

748 The main results of this study may be summarized as follows:

749

750 1. moderate and elevated values of V and Ni in the aerosol were unambiguously
751 associated with the ship source; this attribution was based on:

752 - the V to Ni ratio, which corresponds to what expected for heavy fuel oil
753 combustion;

754 - low amounts of La and Ce with respect to V, and La/Ce ratio similar to those in
755 the UCC, which allowed to exclude power plants or refineries as sources
756 significantly contributing to the observed aerosol;

757 - coincidences between air mass trajectories and travelling ships;

758 2. in addition to travelling ships, also the planetary boundary layer vertical structure
759 played an important role in determining the dispersion of aerosols from the ship
760 source; temperature inversions appeared associated with elevated amounts of ship
761 emissions tracers, suggesting that they favoured the build-up of aerosol
762 concentration in the lowest atmospheric layers;

763 3. as expected, merchant ships (cargo and tankers) appeared to produce a larger
764 impact on the measured aerosol than fishing vessels;

765

766 4. lower limits for the ratios nssSO_4^{2-}/V , NO_3^-/V , and OC/V , identifying the ship-
767 dominated emission cases, were derived from the observations. The lower limits
768 found at Lampedusa, which may be taken as a background site less affected by
769 other types of anthropic emissions, are respectively 207, 12.5, and 44.1. These
770 lower limits are expected to be season dependent;

771

772 5. by using these ratios, the lower limits to the contribution of the ship source to
773 nssSO_4^{2-} , NO_3^- , OA, and to PM_{10} during the measurement campaign were estimated.
774 Ship emissions contributed by at least 34% to the total amount of sulfate, by at
775 least 5-9% to the total amount of NO_3^- , and by at least 9-15% to the total amount
776 of organic aerosol. All these contributions correspond at least to 11% of PM_{10} at LMP
777 ($2.0 \mu\text{g}/\text{m}^3$), and about 8.6% of PM_{10} at CGR ($3.0 \mu\text{g}/\text{m}^3$). In cases with largest ship
778 impact, ships contributed up to about $12 \mu\text{g}/\text{m}^3$ to PM_{10} in both sites, corresponding
779 to 50% of PM_{10} at LMP and 42% at CGR;

780

781 6. Lampedusa is a small island in the southern sector of the central Mediterranean,
782 relatively far from the main shipping Mediterranean route; thus, results at
783 Lampedusa may be taken as representative of the impact of ships on the aerosol
784 properties in a wide open sea area in the central Mediterranean during summer.

785

786

787 **Acknowledgements**

788

789 Measurements at Lampedusa were partly supported by the Italian Ministry for
790 University and Research through the NextData and Ritmare projects.

791 We thank the Institute for Coastal Marine Environment of the National Research Council
792 (IAMC-CNR), for hosting the instruments at Capo Granitola. Thanks are due to
793 MarineTraffic (www.marinetraffic.com) for providing the information on the ship traffic
794 in the Sicily Channel.

795

796

797 **References**

798

799 Agrawal, H., Malloy, Q.G.J., Welch, W.A., Miller, J.W., and Cocker, D.R.: In-use gaseous
800 and particulate matter emissions from a modern ocean going container vessel,
801 *Atmos. Environ.*, 42, 5504–5510, 2008a.

802 Agrawal, H., Welch, W.A., Miller, J.W., and Cocker, D.R.: Emission measurements from
803 a crude oil tanker at sea, *Environ. Sci. Technol.*, 42, 7098–7103, 2008b.

804 Artuso, F., Chamard, P., Piacentino, S., Sferlazzo, D.M., De Silvestri, L., di Sarra, A.,
805 Meloni, D., and Monteleone, F.: Influence of transport and trends in atmospheric CO₂
806 at Lampedusa, *Atmos. Environ.*, 43, 3044–3051, 2009.

807 Ault, A. P., Gaston, C. J., Wang, Y., Dominguez, G., Thiemens, M. H., and Prather, K.
808 A.: Characterization of the single particle mixing state of individual ship plume
809 events measured at the port of Los Angeles, *Environ. Sci. Technol.*, 44, 1954–1961,
810 2010.

811 Becagli, S., Lazzara, L., Fani, F., Marchese, C., Traversi, R., Severi, M., di Sarra, A.,
812 Sferlazzo, D., Piacentino, S., Bommarito, C., Dayan, U., and Udisti, R.: Relationship
813 between methanesulfonate (MS-) in atmospheric particulate and remotely sensed
814 phytoplankton activity in oligo-mesotrophic Central Mediterranean Sea, *Atmos.*
815 *Environ.*, 79, 681–688, 2013.

816 Becagli, S., Sferlazzo, D. M., Pace, G., di Sarra, A., Bommarito, C., Calzolari, G., Ghedini,
817 C., Lucarelli, F., Meloni, D., Monteleone, F., Severi, M., Traversi, R., and Udisti, R.:
818 Evidence for heavy fuel oil combustion aerosols from chemical analyses at the island
819 of Lampedusa: a possible large role of ships emissions in the Mediterranean, *Atmos.*
820 *Chem. Phys.*, 12, 3479–3492, doi:10.5194/acp-12-3479-2012, 2012.

821 Bove, M. C., Brotto, P., Calzolari, G., Cassola, F., Cavalli, F., Fermo, P., Hjorth, J.,
822 Massabò, D., Nava, S., Piazzalunga, A., Schembari, C., and Prati, P.: PM₁₀ source
823 apportionment applying PMF and chemical tracer analysis to ship-borne
824 measurements in the Western Mediterranean, *Atmos. Environ.*, 125, 140–151,
825 doi:10.1016/j.atmosenv.2015.11.009, 2016.

826 Bove, M. C., Brotto, P., Cassola, F., Cuccia, E., Massabò, D., Mazzino, A., Piazzalunga,
827 A., and Prati, P.: An integrated PM_{2.5} source apportionment study: Positive Matrix

828 Factorization vs. the Chemical Transport Model CAMx, *Atmos. Environ.*, 94, 274–
829 286, doi:10.1016/j.atmosenv.2014.05.039, 2014.

830 Bozlaker, A., Buzcu-Güven, B., Fraser, M.P., and Chellam, S.: Insights into PM10 source
831 in Houston, Texas: Role of Petroleum refineries in enriching lanthanoid metal during
832 episodic emission events. *Atmos. Environ.*, 69, 109–117, 2013.
833 doi:10.1016/j.atmosenv.2012.11.068.

834 Bowen, H. J. M.: *Environmental chemistry of the elements*, Academic Press, 1979.

835 Calzolari, G., Nava, S., Lucarelli, F., Chiari, M., Giannoni, M., Becagli, S., Traversi, R.,
836 Marconi, M., Frosini, D., Severi, M., Udisti, R., di Sarra, A., Pace, G., Meloni, D.,
837 Bommarito, C., Monteleone, F., Anello, F., and Sferlazzo, D.M.: Characterization of
838 PM10 sources in the central Mediterranean, *Atmos. Chem. Phys.*, 15, 13939–13955,
839 2015.

840 Canepari, S., Farao, C., Marconi, E., Giovannelli, C., and Perrino, C.: Qualitative and
841 quantitative determination of water in airborne particulate matter, *Atmos. Chem.*
842 *Phys.*, 13, 1193–1202, doi:10.5194/acp-13-1193-2013, 2013.

843 Casasanta, G., di Sarra, A., Meloni, D., Monteleone, F., Pace, G., Piacentino, S., and
844 Sferlazzo, D.: Large aerosol effects on ozone photolysis in the Mediterranean.
845 *Atmos. Environ.*, 45, 3937–3943, 2011.

846 Cassola, F., Ferrari, F., Mazzino, A., and Miglietta, M. M.: The role of the sea on the
847 flash floods events over Liguria (northwestern Italy), *Geophys. Res. Lett.*, 43,
848 doi:10.1002/2016GL068265, 2016.

849 Cesari, D., Genga, A., Ielpo, P., Siciliano, M., Mascolo, G., Grasso, F.M., and Contini, D.:
850 Source apportionment of PM2.5 in the harbour–industrial area of Brindisi (Italy):
851 Identification and estimation of the contribution of in-port ship emissions, *Sci. Total*
852 *Environ.*, 497–498, 392–400, 2014.

853 Chen, G., Huey, G., and Trainer, M.: An investigation of the chemistry of ship emission
854 plumes during ITCT 2002, *J. Geophys. Res.*, 110, D10S90,
855 doi:10.1029/2004JD005236., 2005.

856 Coakley Jr., J. A. and Walsh, C. D.: Limits to the aerosol indirect radiative effect derived
857 from observations of ship tracks, *J. Atmos. Sci.*, 59, 668–680, 2002.

858 Contini, D., Gambaro, A., Belosi, F., Pieri, S.D., Cairns, W.R.L., Donato, A., Zanotto, E.,
859 and Citron, M.: The direct influence of ship traffic on atmospheric PM2.5, PM10 and
860 PAH in Venice, *J. of Environ. Management*, 92, 2119–2129, 2011.

861 Cooper, D.A.: Exhaust emissions from ships at berth, *Atmos. Environ.*, 37, 3817–3830,
862 2003.

863 Corbett, J.J., Winebrake, J.J., Green, E.H., Kasibhatla, P., Eyring, V., and Lauer, A.:
864 Mortality from Ship Emissions: A Global Assessment, *Environ. Sci., Technol.*, 41,
865 8512–8518, doi:10.1021/es071686z, 2007.

866 Dabdub, D., Air quality impacts of ship emission in south coast air basin of California.
867 Final report for State of California Air Resources Board Planning and Technical
868 support division, 2008.

869 Denjean, C., Cassola, F., Mazzino, A., Triquet, S., Chevaillier, S., Grand, N., Bourriane,
870 T., Momboisse, G., Sellegri, K., Schwarzenbock, A., Freney, E., Mallet, M., and

871 Formenti, P.: Size distribution and optical properties of mineral dust aerosols
872 transported in the western Mediterranean, *Atmos. Chem. Phys.*, 16, 1081-1104,
873 doi:10.5194/acp-16-1081-2016, 2016.

874 Derwent, R., Stevenson, D. S., Doherty, R. M, Collins, W. J., Sanderson, M. G., Amann,
875 M., and Dentener, F.: The contribution from ship emissions to air quality and acid
876 deposition in Europe, *Ambio*, 34, 54–59, 2005.

877 Devasthale, A., Krüger, O., and Graßl, H.: Impact of ship emissions on cloud properties
878 over coastal areas, *Geophys. Res. Lett.*, 33, L02811, doi:10.1029/2005GL024470,
879 2006.

880 Diesch, J.M, Drewnick, F., Klimach, T., and Borrmann, S.: Investigation of gaseous and
881 particular emissions from various marine vessel types measured on the banks of the
882 Elbe in Northern Germany, *Atmos. Chem. and Phys.*, 13, 3603–3618, 2013.

883 di Sarra, A., Di Biagio, C., Meloni, D., Monteleone, F., Pace, G., Pugnaghi, S., and
884 Sferlazzo, D.: Shortwave and longwave radiative effects of the intense Saharan dust
885 event of 25-26 March, 2010, at Lampedusa (Mediterranean sea), *J. Geophys. Res.*,
886 116, D23209, doi: 10.1029/2011JD016238, 2011.

887 di Sarra, A., Sferlazzo, D., Meloni, D., Anello, F., Bommarito, C., Corradini, S., De
888 Silvestri, L., Di Iorio, T., Monteleone, F., Pace, G., Piacentino, S., and Pugnaghi, S.:
889 Empirical correction of MFRSR aerosol optical depths for the aerosol forward
890 scattering and development of a long-term integrated MFRSR-Cimel dataset at
891 Lampedusa, *Appl. Opt.*, 54, 2725-2737, 2015.

892 Donateo, A., Gregoris, E., Gambaro, A., Merico, A., Giua, R., Nocioni, A., and Contini,
893 D.: Contribution of harbour activities and ship traffic to PM_{2.5}, particle number
894 concentrations and PAHs in a port city of the Mediterranean Sea (Italy), *Environ. Sci.*
895 *Pollut. Res.*, 21, 9415–9429, doi:10.1007/s11356-014-2849-0, 2014.

896 Du, I., and Turner, J.: Using PM_{2.5} lanthanoid elements and nonparametric wind
897 regression to track petroleum refinery FCC emissions. *Sci. Total. Environ.*, 529, 65-
898 71, doi:10.1016/j.scitotenv.2015.05.034, 2015.

899 Endresen, Ø., Sørsgård, E., Sundet, J. K., Dalsøren, S. B., Isaksen, I. S. A., Berglen, T.
900 F., and Gravir, G.: Emissions from international sea transportation and
901 environmental impact, *J. Geophys. Res.*, 108, 4560, doi:10.1029/2002JD002898,
902 2003.

903 Environmental Modeling Center: The GFS Atmospheric Model. NCEP Office Note 442.
904 National Oceanic and Atmospheric Administration, 2003.

905 Eyring, V., Koehler, H.W., van Aardenne, J., and Lauer, A.: Emissions from international
906 shipping: 1. The last 50 years, *J. Geophys. Res.*, 110, D17305,
907 doi:10.1029/2004JD005619, 2005.

908 Gariazzo, C., Papaleo, V., Pelliccioni, A., Calori, G., Radice, P., and Tinarelli, G.:
909 Application of a Lagrangian particle model to assess the impact of harbour, industrial
910 and urban activities on air quality in the Taranto area, Italy, *Atmos. Environ.*, 41,
911 6432-6444, 2007.

912 Grewal, D., and Haugstetter, H.: Capturing and sharing knowledge in supply chains in
913 the maritime transport sector: critical issues, *Maritime Policy & Management*, 169-
914 183, 2007.

915 Hellebust, S., Allanic, A., O'Connor, I.P., Jourdan, C., Healy, D., and Sodeau, J.R.:
916 Sources of ambient concentrations and chemical composition of PM_{2.5-0.1} in Cork
917 Harbour, Ireland, *Atmos. Res.*, 95, 136-149. 2010.

918 Henderson, P. and Henderson, G. M.: *The Cambridge Handbook of Earth Science Data*,
919 Cambridge, University Press, Cambridge, 42–44, 2009.

920 Henne, S., Brunner, D., Folini, D., Solberg, S., Klausen, J., and Buchmann, B.:
921 Assessment of parameters describing representativeness of air quality in-situ
922 measurement sites, *Atmos. Chem. Phys.*, 10, 3561–3581, 2010

923 Isakson, J., Persson, T.A., and Lindgren, E.S.: Identification and assessment of ship
924 emissions and their effects in the harbour of Goteborg, Sweden, *Atmos. Environ.* 35,
925 3659-3666. 2001.

926 Jiang, Q., Smith, R.B., and Doyle, J.: The nature of the mistral: Observation and
927 modelling of two MAP events, *Q. J. R. Meteorol. Soc.*, 129, 857–875, 2003.

928 Jonsson, A.M, Westerlund, J., and Hallquist, M.: Size-resolved particle emission factors
929 for individual ships, *Geophys. Res. Let.*, 38, L13809. DOI: 10.1029/2011GL047672,
930 2011.

931 Kouvarakis, G., Tsigaridis, K., Kanakidou, M., and Mihalopoulos, N.: Temporal variations
932 of surface regional background ozone over Crete Island in the southeast
933 Mediterranean, *J. Geophys. Res.*, 105, 4399–4407, 2000.

934 Kulkarni, P., Chellam, S., and Fraser, M.P.: Lanthanum and lanthanides in atmospheric
935 fine particles and their apportionment to refinery and petrochemical operations in
936 Houston, TX, *Atmos. Environ.*, 40, 508-520, doi:10.1016/j.atmosenv.2005.09.063,
937 2006.

938 Lauer, A., Eyring, V., Hendricks, J., Jöckel, P., and Lohmann, U.: Global model
939 simulations of the impact of ocean-going ships on aerosols, clouds, and the radiation
940 budget, *Atmos. Chem. Phys.*, 7, 5061–5079, doi:10.5194/acp-7-5061-2007, 2007.

941 Li, Z. and Aneja, V. P.: Regional analysis of cloud chemistry at high elevations in the
942 eastern United States, *Atmos. Environ.*, 26A, 2001–2017, 1992.

943 Lloyd's Register Engineering Services, 1995. *Marine Exhaust Emissions Research*
944 *Programme*, London. pp. 63.

945 Lyyränen, J., Jokiniemi, J., Kauppinen, E.I., and Joutsensaari, J.: Aerosol
946 characterisation in medium-speed diesel engines operating with heavy fuel oils, *J.*
947 *Aerosol Sci.*, 30, 771–784, 1999.

948 Mailler S., Menut, L., di Sarra, A. G., Becagli, S. Di Iorio, T., Bessagnet, B., Briant, R.,
949 Formenti, P., Doussin, J.-F., Gómez-Amo, J. L., Mallet, M., Rea, G., Siour, G.,
950 Sferlazzo, D. M., Traversi, R., Udisti, R., and Turquety, S.: On the radiative impact of
951 aerosols on photolysis rates: comparison of simulations and observations in the
952 Lampedusa island during the ChArMEx/ADRI-MED campaign, *Atmos. Chem. Phys.*,
953 16, 1219–1244, doi:10.5194/acp-16-1219-2016, 2016.

954 Mallet, M., Dulac, F., Formenti, P., Nabat, P., Sciare, J., Roberts, G., Pelon, J., Ancellet,
955 G., Tanré, D., Parol, F., Denjean, C., Brogniez, G., di Sarra, A., Alados-Arboledas, L.,
956 Arndt, J., Auriol, F., Blarel, L., Bourrienne, T., Chazette, P., Chevaillier, S., Claeys,
957 M., D'Anna, B., Derimian, Y., Desboeufs, K., Di Iorio, T., Doussin, J.-F., Durand, P.,
958 Féron, A., Freney, E., Gaimoz, C., Goloub, P., Gómez-Amo, J. L., Granados-Muñoz,
959 M. J., Grand, N., Hamonou, E., Jankowiak, I., Jeannot, M., Léon, J.-F., Maillé, M.,
960 Mailler, S., Meloni, D., Menut, L., Momboisse, G., Nicolas, J., Podvin, T., Pont, V.,
961 Rea, G., Renard, J.-B., Roblou, L., Schepanski, K., Schwarzenboeck, A., Sellegri, K.,
962 Sicard, M., Solmon, F., Somot, S., Torres, B., Totems, J., Triquet, S., Verdier, N.,
963 Verwaerde, C., Waquet, F., Wenger, J., and Zapf, P.: Overview of the Chemistry-
964 Aerosol Mediterranean Experiment/Aerosol Direct Radiative Forcing on the
965 Mediterranean Climate (ChArMEx/ADRIMED) summer 2013 campaign, *Atmos. Chem.*
966 *Phys.*, 16, 455-504, doi:10.5194/acp-16-455-2016, 2016.

967 Marconi, M., Sferlazzo, D.M., Becagli, S., Bommarito, C., Calzolari, G., Chiari, M., di Sarra
968 A., Ghedini, C., Gómez-Amo, J.L., Lucarelli F., Meloni D., Monteleone F., Nava S.,
969 Pace G., Piacentino S., Rugi F., Severi M., Traversi R., and Udisti R.: Saharan dust
970 aerosol over the central Mediterranean Sea: PM₁₀ chemical composition and
971 concentration versus optical columnar measurements, *Atmos. Chem. Phys.*, 14,
972 2039–2054, 2014.

973 Marmer, E. and Langmann, B.: Impact of ship emissions on Mediterranean summertime
974 pollution and climate: A regional model study, *Atmos. Environ.*, 39, 4659–4669,
975 2005.

976 Marmer, E., Dentener, F., Aardenne, J.V., Cavalli, F., Vignati, E., Velchev, K., Hjorth,
977 J., Moldanová, J., Fridell, E., Popovicheva, O., Demirdjian, B., Tishkova, V.,
978 Faccinnetto, A., Focsa, C.: Characterisation of particulate matter and gaseous
979 emissions from a large ship diesel engine, *Atmos. Environ.*, 43, 2632–2641, 2009.

980 Mazzei F., D'Alessandro, A., Lucarelli, F., Nava, S., Prati, P., Valli, G., and Vecchi R.:
981 Characterization of particulate matter sources in an urban environment, *Sci. Tot.*
982 *Environ.*, 401, 81–89, 2008.

983 Mentaschi, L., Besio, G., Cassola, F., and Mazzino, A.: Performance evaluation of
984 WavewatchIII in the Mediterranean Sea, *Ocean Model.*, 90, 82–94,
985 doi:10.1016/j.ocemod.2015.04.003, 2015.

986 Micco, A., and Pérez, N.: Maritime transport costs and port efficiency. In: Bank, I.-A.D.
987 (Ed.), *Inter-american Development Bank*, Santiago de Chile, p. 50. 2001.

988 Mihalopoulos, N., Stephanou, E., Kanakidou, M., Pilitsidis, S. and Bousquet, P.:
989 Tropospheric aerosol ionic composition in the Eastern Mediterranean region, *Tellus*,
990 49B, 1 - 13, 1997.

991 Moldanová, J., Fridell, E., Popovicheva, O., Demirdjian, B., Tishkova, V., Faccinnetto, A.,
992 and Focsa, C.: Characterisation of particulate matter and gaseous emissions from a
993 large ship diesel engine, *Atmos. Environ.*, 43, 2632–2641, 2009.

994 Moreno, T., Querol, X., Alastuey, A., Pey, J. Cruzmiguillon, M., Perez, N., Bernabe, R.,
995 Blanco, S. Cardenas, B., and Gibbons, W.: Lanthanoid geochemistry of urban
996 atmospheric particulate matter, *Environ. Sci. Technol.*, 42, 6502–6507, 2008a.

997 Moreno, T., Querol, X., Alastuey, A., and Gibbons, W.: Identification of FCC refinery
998 atmospheric pollution events using lanthanoid- and vanadium-bearing aerosols.
999 *Atmos. Environ.*, 42, 7851-7861, doi:10.1016/j.atmosenv.2008.07.013, 2008b.

1000 Moreno, T., Querol, X., Castillo, S., Alastuey, A., Cuevas, E., Herrmann, L., Mounkaila,
1001 M., Elvira, J., and Gibbons, W.: Geochemical variation in aeolian mineral particles
1002 from the Sahara-Sahel dust corridor, *Chemosphere*, 65, 261-270,
1003 doi:10.1016/j.chemosphere.2006.02.052 2006..

1004 Murphy, S., Agrawal, H., Sorooshian, A., Padró, L.T., Gates, H., Hersey, S., Welch, W.
1005 A., Jung, H., Miller, J. W., Cocker, D.R. III, Nenes, A., Jonsson, H.H., Flagan, R.C.,
1006 and Seinfeld, J.H.: Comprehensive simultaneous shipboard and airborne
1007 characterization of exhaust from a modern container ship at sea, *Environ. Sci.*
1008 *Technol.*, 43, 4626–4640, 2009.

1009 Olmez, I., and Gordon, G.E.: Rare earths: Atmospheric signatures for oil-fired power
1010 plants and refineries, *Science*, 6, 966–968, 1985.

1011 Pandolfi, M., Gonzalez-Castanedo, Y., Alastuey, A., Rosa, J.d.l., Mantilla, E., Campa,
1012 A.S.d.l., Querol, X., Pey, J., Amato, F., and Moreno, T.: Source apportionment of
1013 PM₁₀ and PM_{2.5} at multiple sites in the strait of Gibraltar by PMF: impact of shipping
1014 emissions, *Environ. Sci. Pollution Res.*, 18, 260-269, 2011.

1015 Schembari, C., Bove, M. C., Cuccia, E., Cavalli, F., Hjorth, J., Massabò, D., Nava, S.,
1016 Udisti, R., and Prati, P.: Source apportionment of PM₁₀ in the Western
1017 Mediterranean based on observations from a cruise ship, *Atmos. Environ.*, 98, 510-
1018 518, 2014.

1019 Sellitto, P., Zanetel, C., di Sarra, A., Salerno, G., Tapparo, A., Meloni, D., Pace, G.,
1020 Caltabiano, T., Briole, P., and Legras, B.: The impact of Mount Etna sulfur emissions
1021 on the atmospheric composition and aerosol properties in the central Mediterranean:
1022 a statistical analysis over the period 2000-2013 based on observations and
1023 Lagrangian modelling, *Atmos. Environ.*, 148, 77-88, 2017.

1024 Shah, S.D., Cocker, D.R., Miller, J.W., and Norbeck, J.M.: Emission rates of particulate
1025 matter and elemental and organic carbon from in-use diesel engines, *Environ. Sci.*
1026 *Technol.*, 38, 2544–2550, 2004.

1027 Simo, R., Colom-Altes, M., Grimalt, J. O. and Albaiges, J.: Background levels of
1028 atmospheric hydrocarbons, sulphate and nitrate over the Western Mediterranean.
1029 *Atmos. Environ.*, 29, 1487-1500, 1991.

1030 Sippula, O., Hokkinen, J., Puustinen, H., Yli-Pirilä, P., and Jokiniemi J: Comparison of
1031 particle emissions from small heavy fuel oil and wood-fired boilers, *Atmos. Environ.*,
1032 43, 4855–4864, 2009.

1033 Sippula, O., Stengel, B., Sklorz, M., Streibel, T., Rabe, R., Orasche, J., Lintelmann, J.,
1034 Michalke, B., Abbaszade, G., Radischat, C., Gröger, T., Schnelle-Kreis, J., Harndorf,
1035 H., and Zimmermann R.: Particle emissions from a marine engine: chemical
1036 composition and aromatic emission profiles under various operating conditions,
1037 *Environ. Sci. Technol.*, 48, 11721–11729, 2014.

1038 Skamarock, W. C., Klemp, J. B., Dudhia, J., Gill, D. O., Barker, D. M., Huang, X. Z.,
1039 Wang, W., and Powers, J. G.: A Description of the Advanced Research WRF Version

1040 3. Technical report. Mesoscale and Microscale Meteorology Division, NCAR, Boulder,
1041 Colorado, 2008.

1042 Solomos, S., Amiridis, V., Zanis, P., Gerasopoulos, E., Sofiou, F. I., Herekakis, T.,
1043 Brioude, J., Stohl, A., Kahn, R. A., and Kontoes, C.: Smoke dispersion modeling over
1044 complex terrain using high resolution meteorological data and satellite observations
1045 – The FireHub platform, *Atmos. Environ.*, 119, 348-361, 2015.

1046 Stein, A. F., Draxler, R. R., Rolph, G. D., Stunder, B. J. B., Cohen, M. D., and Ngan, F.:
1047 NOAA's HYSPLIT atmospheric transport and dispersion modeling system, *Bull. Amer.
1048 Meteor. Soc.*, 96, 2059-2077, [doi:10.1175/BAMS-D-14-00110.1](https://doi.org/10.1175/BAMS-D-14-00110.1), 2015.

1049 Stern, N.: *The Economics of Climate Change: The Stern Review*. Cambridge and New
1050 York, Cambridge University press. 2007.

1051 Trozzi, C., Vaccaro, R., and Nicolo, L.: Air pollutants emissions estimate from maritime
1052 traffic in the Italian harbours of Venice and Piombino, *Sci. Total Environ.*, 169, 257–
1053 263, 1995.

1054 Tsyro, S. G.: To what extent can aerosol water explain the discrepancy between model
1055 calculated and gravimetric PM₁₀ and PM_{2.5}?, *Atmos. Chem. Phys.*, 5, 515–532, 2005.

1056 Turpin, B.J. and Lim H.J.: Species contributions to PM_{2.5} mass concentrations:
1057 Revisiting common assumptions for estimating organic mass, *Aerosol Sci. Technol.*,
1058 35, 602–610, 2001.

1059 Viana, M., Amato, F., Alastuey, A., Querol, X., Moreno, T., Santos, S.G.D., Herce, M.D.,
1060 and Fernández-Patier, R.: Chemical tracers of particulate emissions from commercial
1061 shipping, *Environ. Sci. Tech.*, 43, 7472-7477, 2009.

1062 Viana, M., Hammingh, P., Colette, A., Querol, X., Degraeuwe, B., de Vlieger, I., van
1063 Aardenne, J.: Impact of maritime transport emissions on coastal air quality in
1064 Europe, *Atmos. Environ.*, 90 96-105, 2014.

1065 Viana, M., Kuhlbusch, T.A.J., Querol, X., Alastuey, A., Harrison, R.M., Hopke, P.K.,
1066 Winiwarter, W., Vallius, M., Szidat, S., Prévôt, A.S.H., Hueglin, C., Bloemen, H.,
1067 Wählín, P., Vecchi, R., Miranda, A.I., Kasper-Giebl, A., Maenhaut, W., and
1068 Hitzenberger, R.: Source apportionment of particulate matter in Europe: a review of
1069 methods and results, *J. Aerosol Sci.*, 39, 827-849, 2008.

1070 World Health Organization (WHO): *Health Effects of Particulate Matter, Policy
1071 Implications for Countries in Eastern Europe, Caucasus and Central Asia*, Regional
1072 office for Europe, Copenhagen, Denmark, 2013.

1074 Wu, C., Huang, X. H. H., Ng, W. M., Griffith, S. M., and Yu, J. Z.: Inter-comparison of
1075 NIOSH and IMPROVE protocols for OC and EC determination: Implications for inter-
1076 protocol data conversion, *Atmos. Meas. Tech. Discuss.*, [doi:10.5194/amt-2016-116](https://doi.org/10.5194/amt-2016-116),
in review, 2016